Manitoba
Energy and Mines
Geological Services

Open File Report OF91-2

Geology of the Leo Lake Area, Flin Flon, Manitoba

By K.J. Ferreira
Winnipeg, 1991

Energy and Mines

Hon. Harold J. Neufeld
Minister

Ian Haugh
Deputy Minister

Geological Services

W.D. McRitchie
Director

This publication is available in large print, audiotape or braille on request

92-03110/

TABLE OF CONTENTS

	Page
INTRODUCTION	1
Location and Access	1
General Geology	1
Previous Work	1
Regional Geology	1
Local Geology	1
LITHOLOGIC UNITS	5
Introduction	5
Felsic Volcanic Rocks	5
(1) Fragmental Rhyolite, rusty weathered, < 5% quartz phenocrysts	5
(2) 'Two-quartz' Rhyodacite-Rhyolite, 5 to 25% bimodally distributed quartz phenocrysts	5
(3) Massive (to Fragmental) Rhyodacite-Rhyolite, < 2% quartz phenocrysts	10
(4) Fragmental Rhyodacite-Rhyolite, 5 to 20% unimodally distributed quartz phenocrysts	10
Intrusive Rocks	10
(5) Gabbro	10
(6) Granodiorite	11
STRUCTURE	13
Planar Fabrics	13
Folds	13
Faults	13
Intrusions	21
ALTERATION	23
MINERALIZATION	24
General	24
Exploration History	24
Characteristics of Mineralization	24
ROCK GEOCHEMISTRY	30
Silicate Whole-Rock Analysis	30
Introduction	30
Sample Collection, Preparation and Analytical Methods	30
Results	30
REE Analysis	37
SUMMARY AND DISCUSSION	41
ACKNOWLEDGEMENTS	45
REFERENCES	46
APPENDIX I: Major element analyses	48
APPENDIX II: Copper and zinc analyses, felsic volcanic rocks	50

FIGURES

Figure 1:	Geology of the Flin Flon-Snow Lake area (modified after Bailes, 1971)	iv
Figure 2:	Location of the Baker Patton felsic complex and associated mineral occurrences (after Gale and Eccles, 1987)	2
Figure 3:	Geology of the Leo Lake area, 1:5 000	in pocket
Figure 4:	Brown fine grained fragment with granular quartz in rhyolitic matrix (unit 1, 10N/148E)	4
Figure 5:	White to light grey lobate siliceous fragment (unit 1, 10N/148E)	4
Figure 6:	Lithophysae (unit 1, 20N/156E)	6
Figure 7:	Photomicrograph of lithophysae	6
Figure 8:	Spherulites (unit 1, 32+50N/147+40E)	7
Figure 9:	Quartz phenocrysts in 'two-quartz' rhyolite (unit 2)	7

Page

Figure 10: Etched drill core, unit 2, showing quartz phenocryst size, abundance and distribution 8
Figure 11: Irregular, light grey lapilli to breccia 8
Figure 12: (a) Photograph of zoned fragments, (b) sketch of same zoned fragments highlighting compositional zones (unit 2, 20N/152+30E) 9
Figure 13: Etched slab, unit 4, showing quartz phenocryst size, abundance and distribution 11
Figure 14: Irregular layering trace (20N/156E) 12
Figure 15: Minor folds (unit 1, 20N/150E) 12
Figure 16: S_3 (unit 1, 20N/157+30E) 14
Figure 17: Folded S_3 (unit 1, 22N/162E) 14
Figure 18: Lower hemispheric projection of poles to beds/layers 15
Figure 19: Lower hemispheric projection of poles to foliation within rock fragments 15
Figure 20: Sketch maps of trenches (20N/160E) 16
Figure 21: Lower hemispheric projection of poles to S_2 17
Figure 22: Lower hemispheric projection of poles to planes of elongation of rock fragments 17
Figure 23: Detailed outcrop map of the area near 10N/148E 18
Figure 24: Lower hemispheric projection of poles to minor fold axes 19
Figure 25: Lower hemispheric projection of poles to S_3 19
Figure 26: Representative minor shear zone (unit 2, 12+50N/143E) 19
Figure 27: Sheared textures in etched slab, unit 4 20
Figure 28: Photomicrograph of (a) nonsheared vs. (b) sheared textures from minor shear zone, unit 4 20
Figure 29: Lower hemispheric projection of poles to shear zones 21
Figure 30: Lower hemispheric projection of poles to quartz ± chlorite veinlets 21
Figure 31: Silica network (unit 1, 20+30N/146+50E) 22
Figure 32: Ovoid 'pseudo-lapilli' in chloritized groundmass (25N/21+40E) 22
Figure 33: Location of diamond drill holes and electromagnetic conductors (modified from Gale and Eccles, 1987) 26
Figure 34: Location of holes drilled on the East Zone by God's Lake Mines Ltd. (Gale and Eccles, 1987) 27
Figure 35: Lapilli tuff with irregular rusty weathered areas (unit 1) 28
Figure 36: Angular sulphide clast in quartz-phenocryst-poor rhyolitic lapilli tuff (unit 1, 20N/147+20E) 28
Figure 37: Sulphide breccia (unit 1, 20N/147+20E) 29
Figure 38: Sample locations of rock geochemical analyses . . . . . in pocket
Figure 39: Contour map of MgO (wt. %) distribution 33
Figure 40: Contour map of Na_2O (wt. %) distribution 34
Figure 41: Contour map of K_2O (wt. %) distribution 35
Figure 42: MgO (wt. %) vs. LOI (wt. %) 36
Figure 43: Contour map of Cu (ppm) concentrations 38
Figure 44: Contour map of Zn (ppm) concentrations 39
Figure 45: Chondrite normalized REE plot of porphyry phase of unit 2 (sample M-34) 40

Page

TABLES

Table 1: Summary of exploration history of the Leo Lake occurrence 25
Table 2: Summary of descriptive statistics for felsic volcanic rocks, Leo Lake area 31
Table 3: Summary of descriptive statistics for unit 1, Leo Lake area 31
Table 4: Summary of descriptive statistics for unit 2, Leo Lake area 31
Table 5: Summary of descriptive statistics for unit 3, Leo Lake area 32
Table 6: Summary of descriptive statistics for unit 4, Leo Lake area 32
Table 7: Spearman correlation coefficient matrix for felsic volcanic rocks, Leo Lake area 32
Table 8: Summary of characteristics of fragments from units 1 through 4 43
Table 9: Main textural criteria for distinguishing true felsic pyroclastic rocks from false pyroclastic rocks (from Allen, 1988), and synopsis of these criteria for the Leo Lake area 44

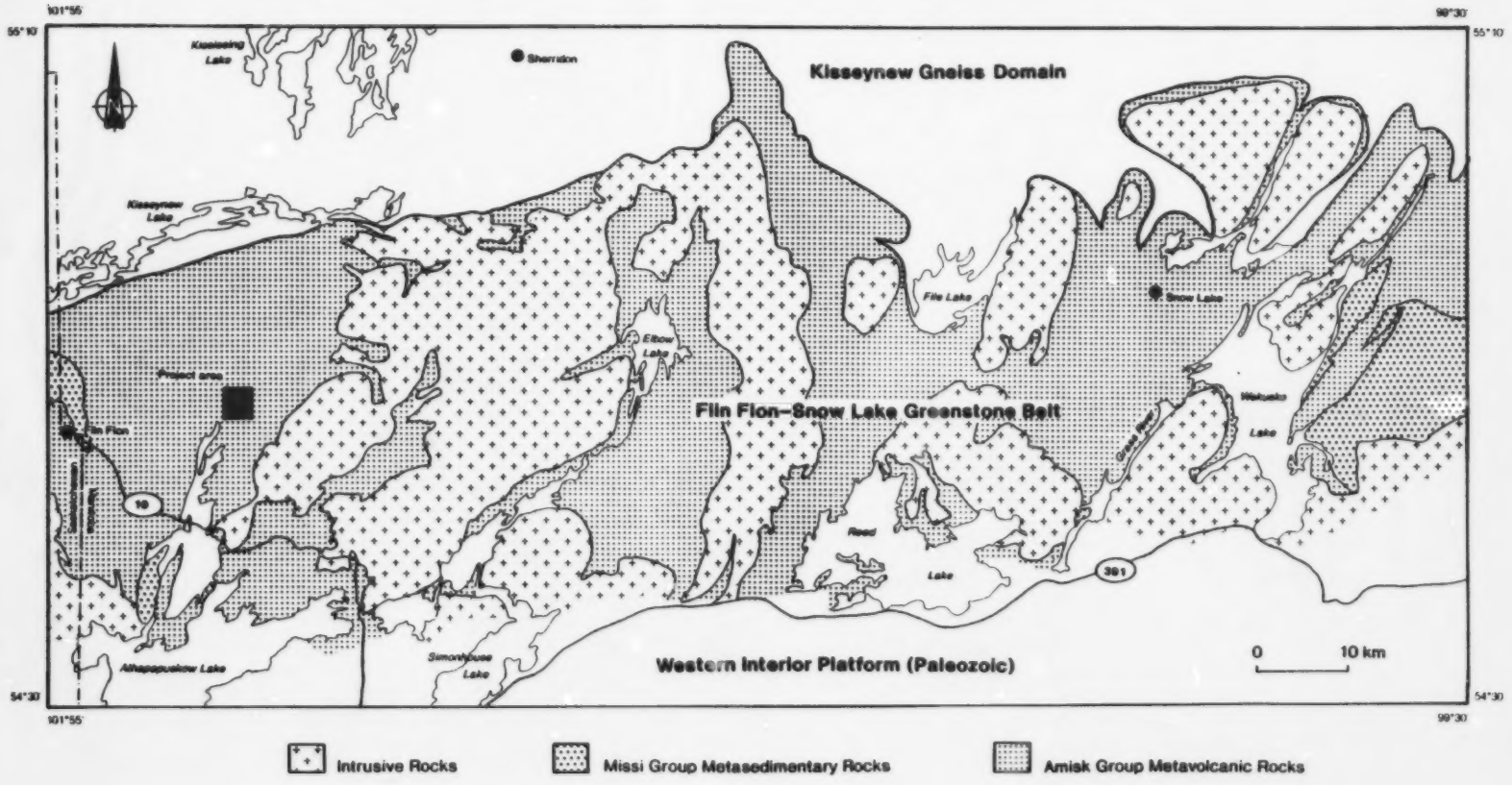

Figure 1: Geology of the Flin Flon-Snow Lake area (modified after Bailes, 1971).

INTRODUCTION

A large complex of felsic volcanic and hypabyssal rocks occupies approximately 15 km^2 centred on Thompson Lake in the Proterozoic Flin Flon-Snow Lake greenstone belt. A number of mineral deposits and occurrences are hosted by these rocks. As part of mineral deposit studies under the Canada-Manitoba Mineral Development Agreement, portions of the Baker Patton felsic complex were selected to be mapped in detail in an attempt to better define the lithologies of these rocks, and their associated alteration and mineralization. This report describes the results of 1:2 500 geological field work and follow-up petrographic, structural and geochemical analyses covering approximately 2 km^2 between Flintoba and Leo lakes. Mapping was carried out over fourteen weeks in the 1987 and 1988 field seasons.

LOCATION AND ACCESS

The project area is located 19 km east of the town of Flin Flon, mainly between Flintoba Lake and Leo Lake (Fig. 1). Access may be gained by vehicle to the end of the North Star Road, which branches northeast from Highway 10A, and then by boat from Thompson Lake through Flintoba Creek to Flintoba Lake. Alternatively, the project area may be reached by all-terrain vehicle along a tractor trail that starts from the North Star Road where it crosses Flintoba Creek.

An exploration grid cut by Granges Exploration Ltd. was used to provide location control within the map area. The grid had been constructed with 200 ft. (61 m) line spacings and 100 ft. (30.5 m) stations; two baselines are oriented at 040°.

Outcrop is fairly abundant within most of the map area, but it is heavily obscured by lichen cover.

GENERAL GEOLOGY

Previous Work

Bateman and Harrison (1945) and Buckham (1940) mapped the area at a scale of one inch to one mile. Recent mapping by Bailes and Syme (1989) at a scale of 1:20 000 covered the southern part of the felsic complex.

Selected areas near massive sulphide deposits within the felsic complex have been described or mapped in detail. Wright (1931, p. 51-52) presented descriptions of the Baker Patton and Don Jon massive sulphide deposits. Geologists from Hudson Bay Mining and Smelting Company Limited presented descriptions of the North Star and Don Jon massive sulphide deposits (1957). Bailes and Lamb mapped the Pine Bay area at a scale of 1:4 800 in 1977 (Manitoba Energy and Mines, unpublished map). The area surrounding the Baker Patton deposit has been mapped at a scale of 1:1 000 (Hayden-Luck and Gale, 1985; Tannahill and Gale, 1986; Gale and Foote, 1988). Geochemical analyses are available for rocks from the area near the Baker Patton deposit (Mwanange'Onze, 1978) and for rocks from the vicinity of the North Star deposit (England, 1979). Preliminary results from field work for the Leo Lake area were summarized by Ferreira (1987a, 1987b, 1988).

Regional Geology

The Thompson Lake area is located in the western portion of the Proterozoic Flin Flon-Snow Lake greenstone belt (Fig. 1). Supracrustal rocks in the greenstone belt are assigned to the predominantly mafic volcanic Amisk Group and the younger, dominantly sedimentary Missi Group (Bruce, 1918).

The Amisk Group consists of dominantly subaqueous basalt to basaltic andesite and associated volcaniclastic rocks (Stauffer *et al.*, 1976). Felsic volcanic and volcaniclastic rocks constitute a comparatively minor component of the Amisk Group, particularly in the western part of the greenstone belt; the Baker Patton felsic complex is notable because it is the largest known mass of felsic volcanic rocks in the Flin Flon area. The Amisk Group also contains minor amounts of oxide facies iron formation, carbonate-rich sedimentary rocks, and cherty graphitic sulphidic sedimentary rocks (Bailes *et al.*, 1987). Amisk Group volcanism has been dated at 1886 ± 2 Ma (Gordon *et al.*, 1990).

The Missi Group lies with angular unconformity upon the Amisk Group. It consists of a variety of clastic rocks, including sandstone, pebbly sandstone and polymictic conglomerate deposited in a terrestrial environment. Felsic volcanic rocks constitute part of the group east of Wekusko Lake in the eastern part of the greenstone belt, but are not present in the Missi Group in the Flin Flon area (Bailes *et al.*, 1987). Missi Group volcanism has been dated at 1832 ± 2 Ma (Gordon *et al.*, 1990).

Rocks in the Flin Flon-Snow Lake greenstone belt have been affected by multiple stages of deformation, regional metamorphism and intrusion of numerous felsic to mafic plutons. Although multiple phases of folding and faulting affected the entire greenstone belt, the western part of the belt is characterized by numerous fault-bounded domains, each of which has distinct stratigraphic and lithologic characteristics that cannot be traced or extrapolated between domains (Bailes and Syme, 1989). Metamorphism in the belt varies from sub-greenschist facies in parts of the Flin Flon area to upper amphibolite facies in the File Lake area. In the Flin Flon area, metamorphism is generally lower to upper greenschist facies. Mafic and felsic plutons have been identified as Amisk, pre-Missi, and post-Missi in age (Bailes and Syme, 1989; Bailes *et al.*, 1987).

Local Geology

Bateman and Harrison (1945) mapped rhyolite, porphyritic dacite, minor rhyolitic tuff and dacitic tuff and breccia, and minor intrusive equivalents in the Thompson Lake area. These felsic rocks extend from Sourdough Bay on Athapapuskow Lake, east to Jenny Lake, and beyond Alberts Lake in the north (Fig. 2). Bailes and Syme (1989) termed these felsic rocks the *Baker Patton felsic complex*, which forms part of the stratigraphic sequence in the Sour-

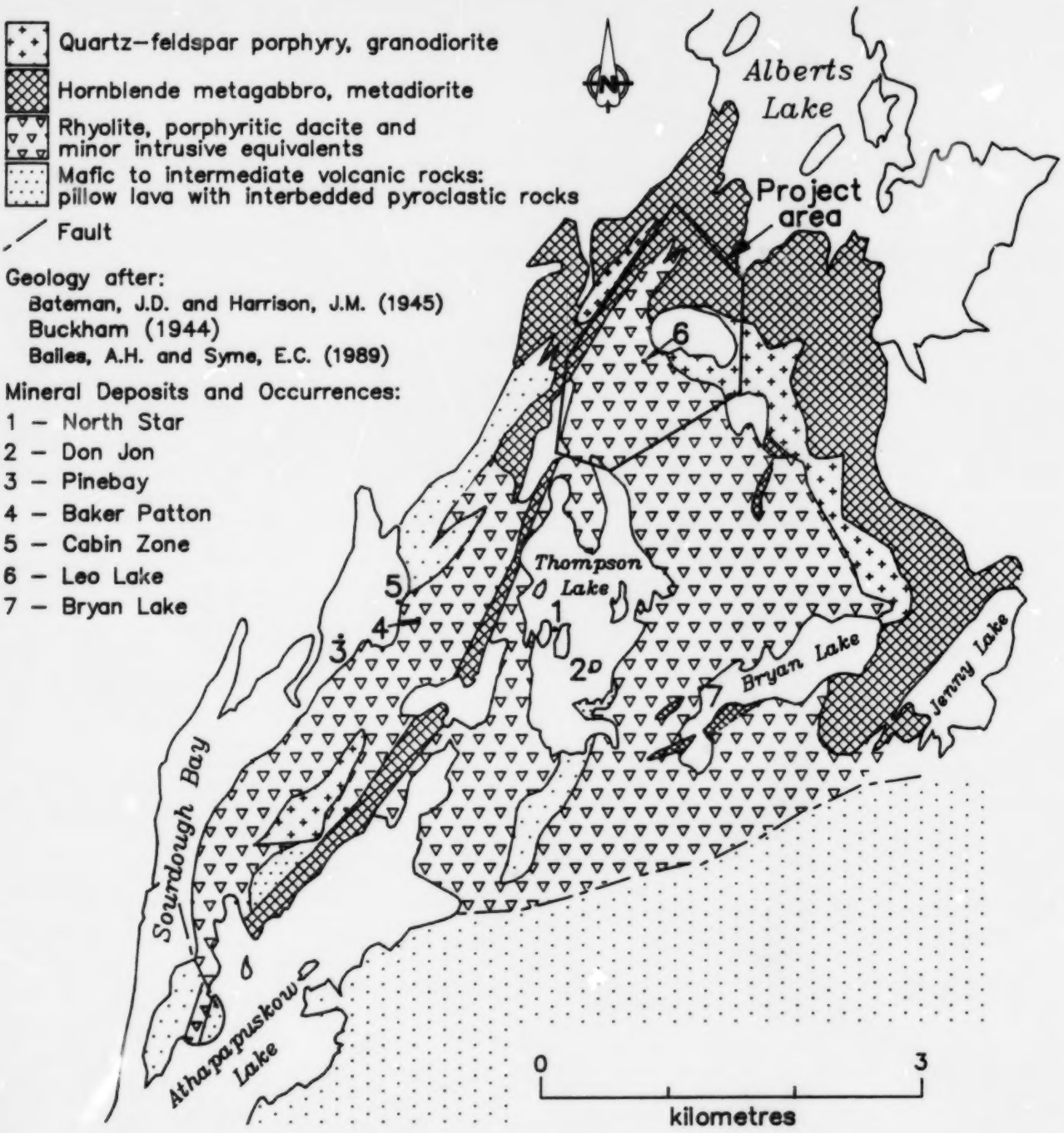

Figure 2: Location of the Baker Patton felsic complex and associated mineral occurrences (after Gale and Eccles, 1987).

dough Bay Fault Block. They described quartz- and plagioclase-phyric dacite to rhyolite dykes, massive felsic rocks, and tuff and lapilli tuff at the southwestern end of the complex.

Approximately 2 km south of Thompson Lake the felsic rocks are in fault contact with intermediate to mafic volcanic rocks (Fig. 2; Buckham, 1944). The felsic rocks are bounded to the north and east by diorite and gabbro, and to the west by intermediate to mafic volcanic and volcaniclastic rocks. Minor felsic intrusions, probably pre-Missi and possibly syndepositional, occur at the northeast edge of, and locally within, the felsic complex. Rocks in the study area have been metamorphosed to lower greenschist facies (biotite absent).

The Baker Patton felsic complex hosts a number of volcanogenic massive sulphide type Cu-Zn deposits and occurrences, which commonly include extensive alteration zones (Fig. 2). Deposits include the North Star, Pinebay, Don Jon, Baker Patton and Cabin Zone; occurrences include Leo Lake and Bryan Lake. Information presented below for these deposits and occurrences is summarized from Gale and Eccles (1988):

The North Star deposit produced 241 643 tonnes averaging 6.11% Cu with 0.27 to 0.41 g/t Au and 6.8 to 10 g/t Ag; it produced ore during 1954-58. The deposit comprised a solid sulphide lens of pyrite and chalcopyrite and a deformed footwall stringer zone. It had a maximum width of 75 m, an average thickness of 6 m, and was mined to the 140 m level. The deposit was hosted by cherty chlorite schist that was chiefly composed of quartz, chlorite and carbonate.

The Don Jon deposit produced 87 283 tonnes averaging 3.06% Cu, 0.96 g/t Au and 15.2 g/t Ag. It was mined between 1954 and 1957, via a crosscut from the North Star mine. The deposit consisted of two solid sulphide lenses hosted by chloritic dacite. The lenses, composed of pyrite and chalcopyrite, were northeast-striking with a 75°NW dip and a steep southwesterly plunge.

The Pinebay deposit has reserves of 1 340 000 tonnes grading 1.5% Cu, including a 400 000 tonne section grading 3.2% Cu. The deposit contains only traces of Au and up to 6 g/t Ag. An exploration shaft has tested the deposit. The deposit consists of four zones of solid sulphide minerals, specifically pyrite, pyrrhotite and chalcopyrite, with minor bornite and sphalerite. The sulphide minerals are hosted by quartz-sericite-carbonate schist that is rich in quartz, sericite, chlorite, talc and Fe-carbonate. The zones are surrounded by chloritic schist or altered chloritic rocks.

The Baker Patton deposit contains an estimated 50 000 tonnes grading 1% Cu. An exploration shaft was sunk to a depth of 126 m. The deposit consists of two zones of solid pyrite and bands of chalcopyrite intimately mixed with pyrite, and two additional zones that contain chalcopyrite ± pyrite vein type mobilizate. The deposit is hosted by intensely altered rhyolite to dacite, and is marked at surface by an extensive conspicuous area of oxidized sulphide mineralization.

The Cabin Zone contains 72 000 tonnes averaging 6.9% Zn and 1% Cu, which is the largest accumulation of Zn mineralization known in the Baker Patton felsic complex. The sulphide body consists of solid pyrite with sphalerite bands, chalcopyrite blebs and stringers, and minor pyrrhotite and magnetite hosted by altered rhyodacitic and rhyolitic rocks. The alteration zone consists of an extensive network of pyrite veins and blebs in sericite-chlorite-quartz schist with minor blebs and veinlets of sphalerite and chalcopyrite.

The Bryan Lake occurrence is characterized by disseminated pyrite, minor chalcopyrite, and narrow stringers and veins of quartz and pyrite hosted by sericitized and chloritized felsic volcanic rocks.

The Leo Lake occurrence is described in this report under 'Mineralization'.

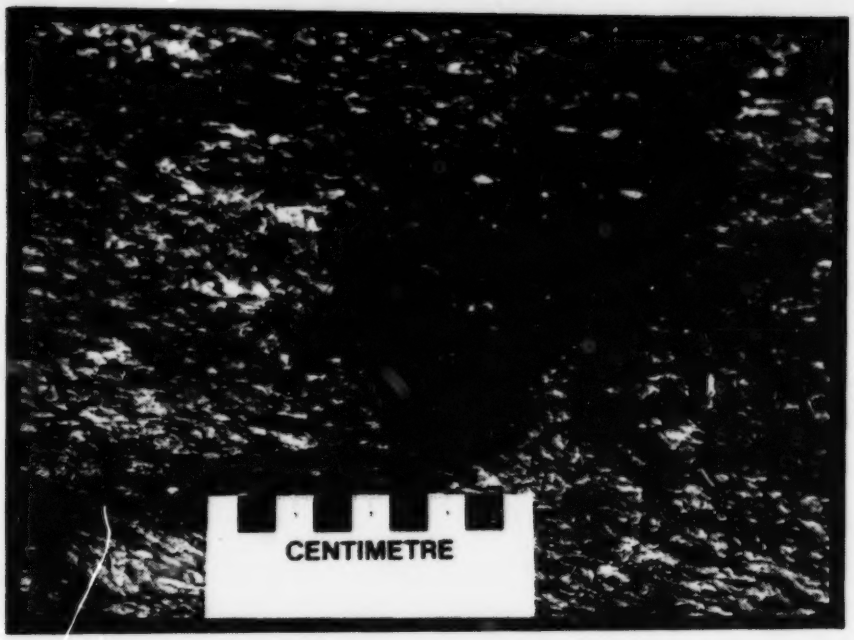

Figure 4: Brown fine grained fragment with granular quartz in rhyolitic matrix (unit 1, 10N/148E).

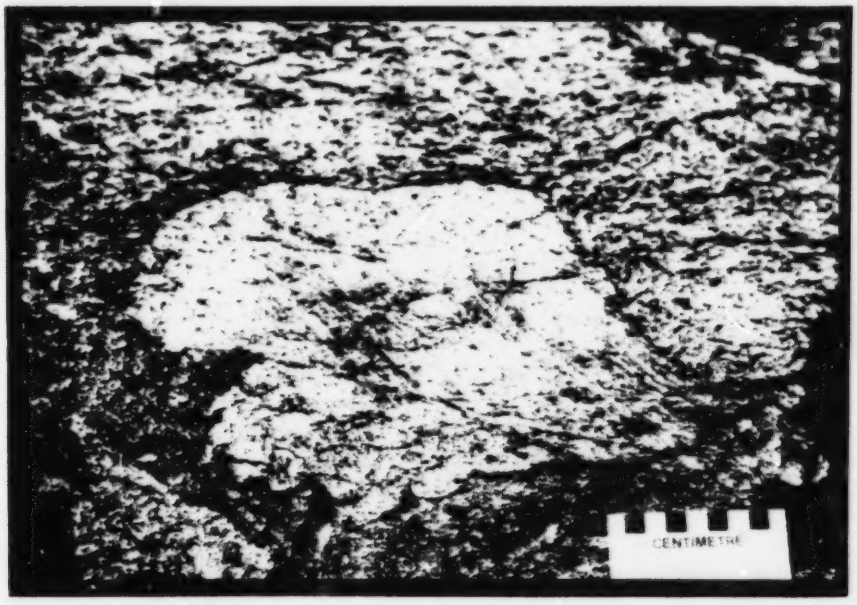

Figure 5: White to light grey lobate siliceous fragment (unit 1, 10N/148E).

LITHOLOGIC UNITS

INTRODUCTION

The majority of the map area is underlain by rhyolitic and rhyodacitic volcanic rocks (Fig. 3, in pocket). Lesser gabbro and granodiorite intrusions are present, particularly in the northern part of the map area. Determination of the size, abundance and distribution of quartz phenocrysts is instrumental in distinguishing different lithologic units among the felsic volcanic rocks. Massive felsic rocks are present, but flow textures were not identified. Fragmental rocks dominate and include tuff, lapilli tuff and tuff breccia. Some strata are monolithologic, others are heterolithologic. Fragments in heterolithologic units are felsic, and differ primarily in their phenocryst content and internal grain size. Since fragments and matrix commonly have similar compositions and textures, it is difficult to distinguish between them on outcrop. Original differences between strata have been further obscured by deformation.

Primary bedding features are rare, and presumably have not been preserved due to alteration and deformation. Stratigraphic tops were not determined and age relationships are uncertain in the study area. Elsewhere in the Sourdough Bay Fault Block, which includes the Baker Patton felsic complex, Bailes and Syme (1989) mapped strata that faces toward the northwest; however, at the Baker Patton deposit stratigraphy faces toward the southeast.

FELSIC VOLCANIC ROCKS

(1) Fragmental Rhyolite, rusty weathered, < 5% quartz phenocrysts

Rusty weathered rhyolite with < 5% quartz and < 5% plagioclase phenocrysts constitute a major portion of the study area (Fig. 3). Quartz phenocrysts, up to 5 mm, generally < 1 mm, are subrounded, anhedral to subhedral, broken, embayed, mono- and polycrystalline, inhomogeneously distributed, and brecciated *in situ*. Plagioclase phenocrysts are up to 1.5 mm, subhedral to anhedral and broken. Lithic fragments are felsic and constitute up to 25% of the rock, but average < 10%. Fragments are mostly angular or lenticular, elongate in the direction of cleavage, but may also be round, tabular, irregular and ovoid. Lithic fragments are ash to blocks, but dominantly ash to fine lapilli, and are commonly internally fragmented. Some fragments contain quartz phenocrysts, many lack phenocrysts. Lithic fragments include: (1) light grey to beige, aphanitic blocks averaging 3 x 10 cm, some of which contain up to 10%, 1 to 3 mm quartz phenocrysts; (2) light brownish, very fine grained, angular (to rounded) blocks from about 10 cm to 60 cm long consisting of abundant granular quartz in a recessively weathered brown matrix (Fig. 4), and a comparatively rare variant in which quartz appears to form partial tubes (possible pumice); (3) buff aphanitic lapilli to blocks up to 2 x 12 cm containing 1% mm-size quartz phenocrysts; and (4) rare clusters of white to light grey, lobate, granular, siliceous blocks from 3 x 13 cm to 17 x 54 cm (Fig. 5). The matrix is creamy beige to light brown with patchy to pervasively rusty weathered areas and an aphanitic, massive to pebbly appearance. The matrix has an average grain size of 0.05 mm and comprises plagioclase, quartz, chlorite and minor Fe-Ti oxide minerals.

Where beds are distinguishable, their contained fragments are heterolithic and polymodal. Tuff layers are usually < 1 m thick.

Abundant round to irregularly shaped structures, 0.3 to 2.5 cm across, constitute up to 2% of outcrops at 20N/156E and 34N/148E (Fig. 6, 7). They have brown, recessively weathered centres surrounded by a bleached rim 2 to 4 mm wide. They do not occur within recognizable lithic fragments, and are confined to the matrix. These structures are interpreted as lithophysae, which indicate that the rocks were vitric and hot. Coalescing spherulites, another indicator of devitrification, are present at 32+50N/147+40E (Fig. 8).

(2) 'Two-quartz' Rhyodacite-Rhyolite, 5 to 25% bimodally distributed quartz phenocrysts

Unit 2 weathers creamy white and in places has a light greenish hue. It is aphanitic and has a pebbly appearance. Quartz phenocrysts compose 5 to 25% of the rock, have bimodal size distribution, and are ≤ 2 mm and 4 to 15 mm across; the phenocrysts in the smaller size range outnumber the larger by a ratio of approximately 2:1. Phenocrysts are subrounded, broken, embayed, monocrystalline and lesser polycrystalline, and some are brecciated *in situ* (Fig. 9, 10). Subhedral to euhedral, tabular and broken phenocrysts form 0 to 10% of the rock. Plagioclase is up to 1.5 mm long in the western part of the unit, but up to 1 cm (average 4 mm) long along the south shore of Leo Lake (2d, Fig. 3). Lithic fragments compose up to 25% of the rock; they are felsic, angular to rounded, heterolithic, and range from ash to blocks, including blocks up to 3 x 5 m. The more prevalent types of fragments are: (1) white, lenticular lapilli and blocks composed of felsic ash and quartz phenocrysts of variable size and abundance (including 'two-quartz' fragments) in a white matrix (Fig. 11), (2) white, lenticular, quartz phenocryst-poor, aphanitic, felsic lapilli, and (3) reddish-brown, angular to rounded, very fine grained, chloritic fragments with up to 10%, < 1 mm quartz phenocrysts(?). A group of unusual, internally zoned fragments (possible bombs) up to 20 cm long are present at 20N/152E (Fig. 12). The matrix consists of altered quartz and plagioclase with an average grain size of 0.05 mm.

Beds are observed only in outcrops near 20N/152E; here, they vary from less than 1 to several metres thick. The fragments are unsorted, unstratified and matrix supported.

Unit 2 rocks directly south of Leo Lake (31+50N/165E; unit 2d, Fig. 3) have a more massive appearance than unit 2 rocks elsewhere in the map area. Lithic fragments are obscure, and where identifiable, they are less abundant, less heterogeneous and smaller. Although fragments were not positively identified in outcrops from this area, they are readily identifiable in thin section, and compose 5% of the

Figure 6: Lithophysae (unit 1, 20N/156E).

Figure 7: Photomicrograph of lithophysae. Chlorite core is surrounded by a fine grained aggregate of quartz. Structure is rimmed with tangential to

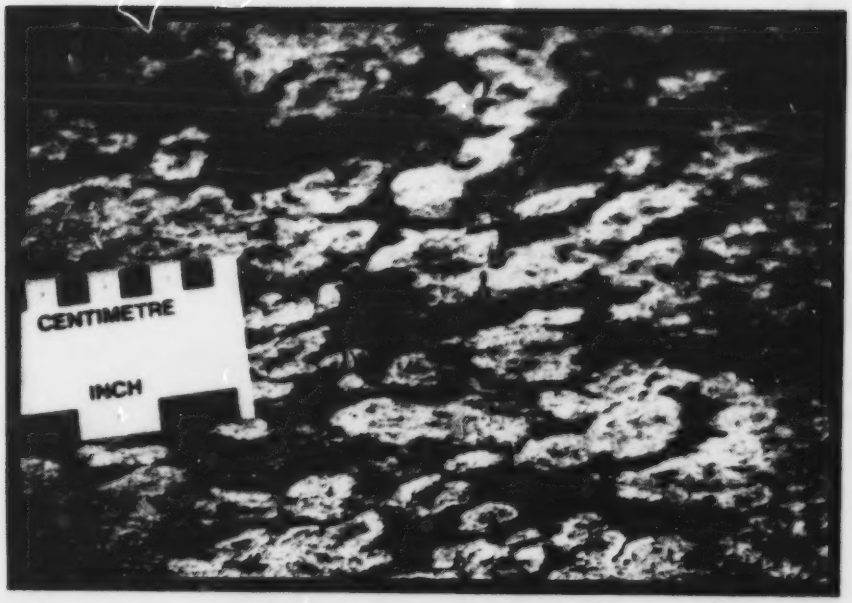

Figure 8: Spherulites (unit 1, 32+50N/147+40E).

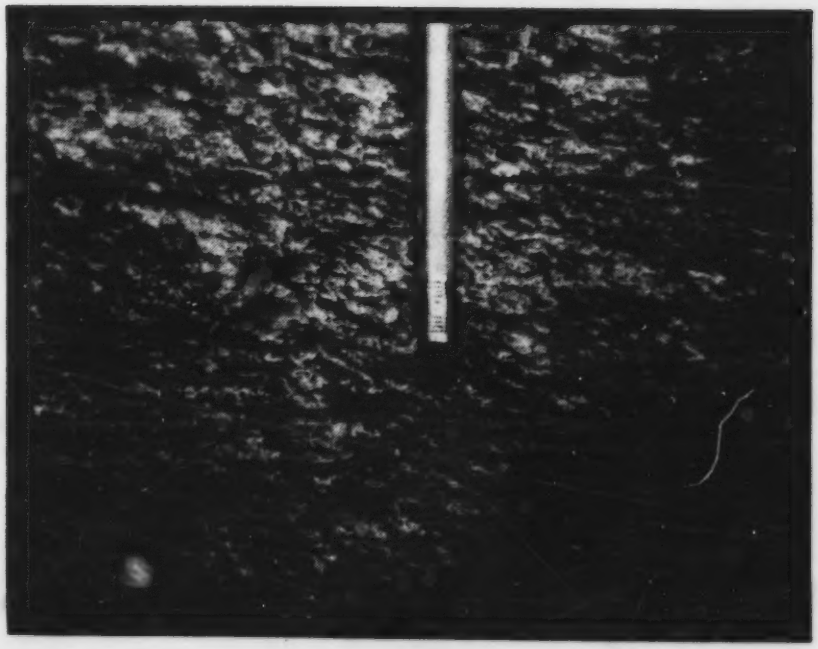

Figure 9: Quartz phenocrysts in 'two-quartz' rhyolite (unit 2).

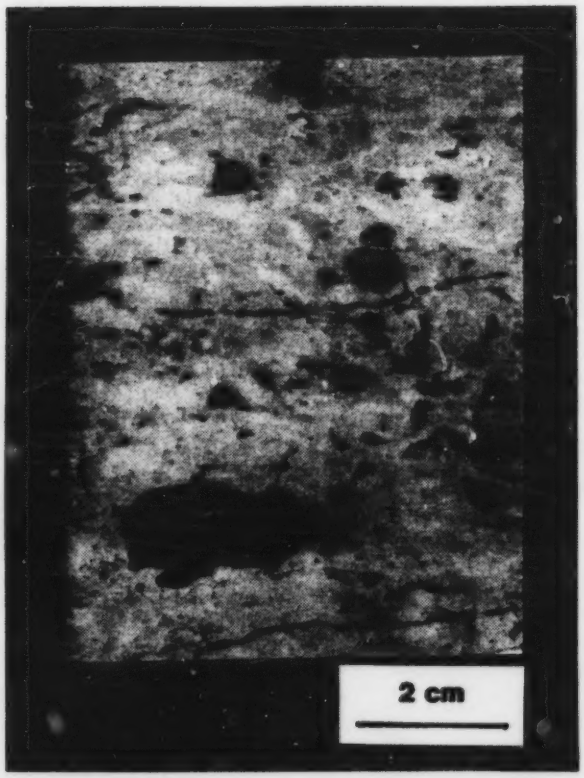

Figure 10:
Etched drill core, unit 2, showing quartz phenocryst size, abundance and distribution.

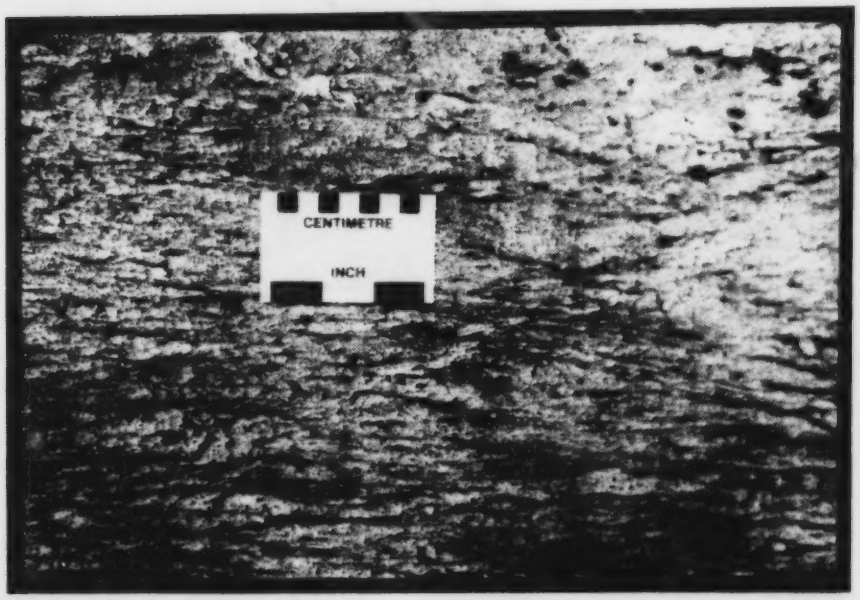

Figure 11: Irregular, light grey lapilli to breccia.

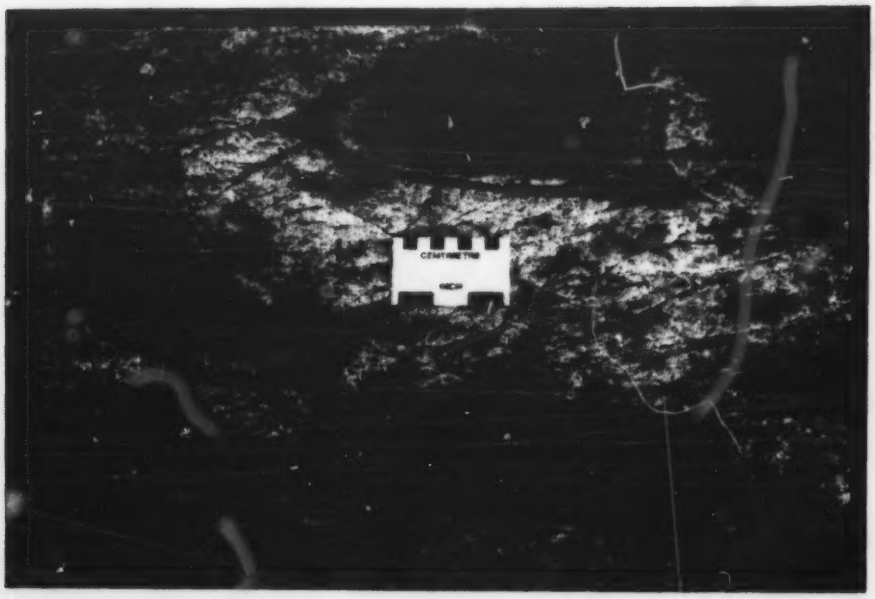

Figure 12(a): Photograph of zoned fragments.

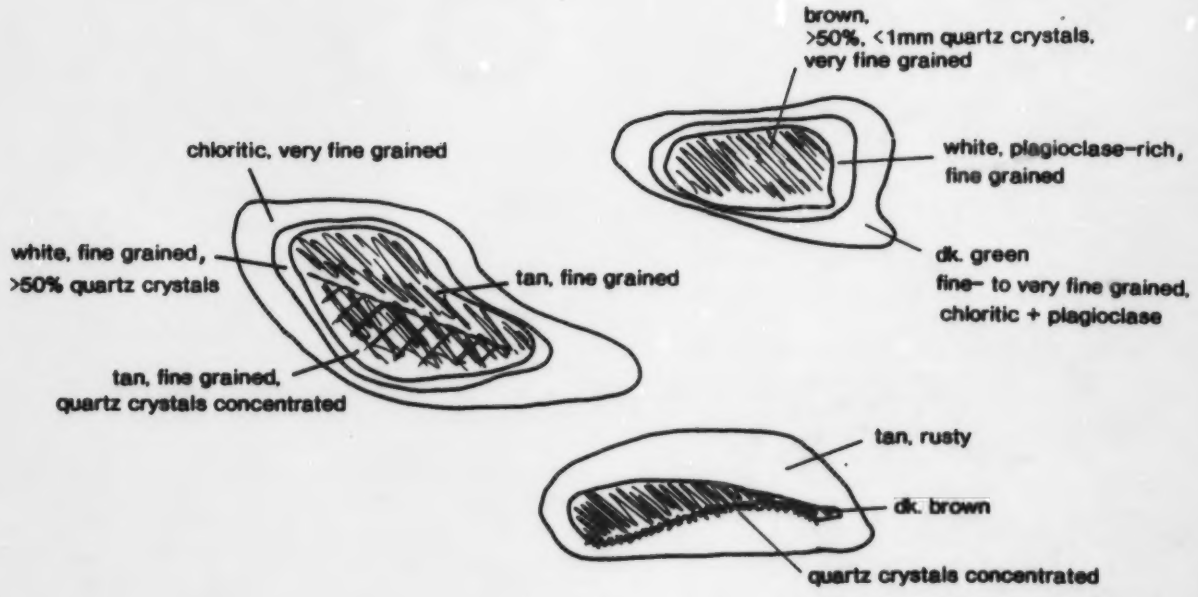

Figure 12(b): Sketch of same zoned fragments highlighting compositional zones (unit 2, 20N/152+30E).

rock. These lapilli have irregular shapes and contain 2 mm, broken, randomly oriented quartz and plagioclase phenocrysts in an aphanitic matrix. The internal composition and texture of the lapilli suggest that they were derived from previously consolidated fragmental deposits. Despite these differences, there are major similarities between these rocks and unit 2 rocks elsewhere in the map area. Quartz phenocrysts have the same distinctive sizes, shape, abundance, and distribution. Matrices have the same composition and grain size. The types of lithic fragments in rocks south of Leo Lake are also present in other unit 2 rocks. Thus, the rocks south of Leo Lake are considered part of unit 2. The local differences suggest that rocks south of Leo Lake may be hypabyssal intrusive equivalents of the 'two-quartz' fragmental rocks elsewhere in the map area.

(3) Massive (to Fragmental) Rhyodacite-Rhyolite, < 2% quartz phenocrysts

Rhyodacitic to rhyolitic rocks with < 2% visible quartz phenocrysts in the northern and southern parts of the map area weather creamy white to creamy beige and in places have a light green or pink hue. A massive blocky appearance is most common, but fragmental textures are present. Where present, quartz phenocrysts are 2 mm across and are inhomogeneously distributed and commonly enclosed within quartz-phyric fragments. Plagioclase, 0 to 1%, occurs as < 1 mm tabular phenocrysts. In places, a fragmental texture is discernible, giving a pebbly appearance to the rock. Fragments are generally monolithic (to heterolithic), aphyric, ash to fine lapilli, and are round to lenticular. In thin section, these fragments are discrete lens-shaped aggregates up to 6 mm long, elongated subparallel to the direction of foliation, and the original mineral assemblage of quartz and feldspar is replaced by sericite. Pinkish-orange fragments are common in the southern part of the map area.

A bedded sequence of quartz-phenocryst-poor tuff, quartz-phenocryst-poor lapilli tuff, quartz-crystal tuff and quartz-phenocryst-poor tuff from south to north occurs at 48N/142E. A separate bedded sequence of quartz-phenocryst-poor tuff, quartz-crystal tuff, to quartz-phenocryst-poor tuff from west to east is present at 52N-54N/144E. The quartz-crystal tuff is at least 2.1 m and up to 5.2 m thick. The contact between the western quartz-phenocryst-poor tuff and the quartz-crystal tuff is sharp, unaltered and slightly undulating in thin section. Within beds, fragments are unsorted, unstratified and matrix supported.

An outcrop at 4S/148E contains 60%, white, round to ovoid, nonaligned, siliceous structures up to 3 cm, but average 2 to 5 mm, that may be spherulites. Clusters of recessively weathered ovoids up to 1 cm long are present at 6N/166+50E. It is possible that these structures may be vesicles or lithophysae, but their origin is unknown.

Massive rocks that are not obviously fragmental may represent hypabyssal intrusions, but the relationship between fragmental and massive areas is not clear. Flow textures and chilled margins were not observed. The genesis of the massive rocks remains unproven.

Outcrops are usually covered with lichen and are sparse in the southern part of the map area. However, similarities in texture and composition suggest these rocks are equivalent to rocks from unit 3 in the northern part of the map area. Rocks near the north end of Flintoba Lake to the west of the major NNE-trending fault are tentatively assigned to unit 3.

(4) Fragmental Rhyodacite-Rhyolite, 5 to 20% unimodally distributed quartz phenocrysts

Unit 4 is aphanitic and weathers creamy white to very light beige, and has a granular or pebbly appearance. These rhyodacitic to rhyolitic rocks contain 5 to 20% embayed euhedral to subhedral quartz phenocrysts. The phenocrysts are up to 10 mm, average 2 mm, broken to rounded, and some are brecciated *in situ* (Fig. 13). They are mostly monocrystalline and only rarely occur as polycrystalline aggregates. Plagioclase, 2 to 15%, occurs as broken single tabular phenocrysts and polycrystalline aggregates averaging 2 mm in length. Quartz and plagioclase phenocrysts are homogeneously to inhomogeneously distributed. Lithic fragments are angular, ovoid and lenticular. They are dominantly ash and lapilli, generally form 1%, but locally form up to 30% of the rock; blocks up to 10 cm long are randomly distributed. Although the lithic fragments are felsic, several types are present: white, aphanitic, massive or fragmental, quartz-phyric or aphyric fragments; and minor, fine grained, dark greenish-brown, recessively weathered fragments.

Beds are rarely distinguishable, but thicknesses from 0.1 m to 4.6 m were measured for individual beds. Beds do not exhibit internal stratification. Reddish-brown discontinuous layers or lenses of tuff, usually < 10 to 20 cm thick, occur at some contacts between beds. At 34N/147+50E, possible pumice fragments, approximately 2 x 20 cm, occur at the contact between a quartz phenocryst-rich layer and phenocryst-poor layer.

INTRUSIVE ROCKS

(5) Gabbro

Gabbro is brown or mottled weathered, massive, nonporphyritic and medium- to coarse-grained. It comprises 50 to 60% plagioclase and 40 to 50% chloritized amphibole. Locally, these rocks may also contain 2 to 5% fine grained quartz, 1 to 2% fine grained magnetite, and 1% epidote that surrounds amphibole phenocrysts and also forms irregular discrete 'pods'. Sheared rocks have a very fine grained granular appearance and contain greater amounts of these accessory minerals. For example, outcrops at 62N/159+50E and 65N/139+50E contain up to 25% quartz and 20% magnetite, in addition to feldspar and amphibole.

In places, late, narrow (generally cm-to dm-wide) mafic dykes are present within the felsic volcanic rocks; they are easily distinguished from chloritic tuff layers by their straight sharp crosscutting contacts with the felsic rocks. They have not been notably altered or structurally distorted.

(6) Granodiorite

Granodiorite is beige weathered and mostly equigranular, averaging 3 to 5 mm. It comprises 15%, clear to grey-white, subhedral quartz, 25% chloritized amphibole (usually hornblende) and 60% plagioclase. Rocks from this unit that occur near the major NNE-trending fault are granulated and are extensively sericitized, chloritized, saussuritized and lightly carbonatized (see 'Structure').

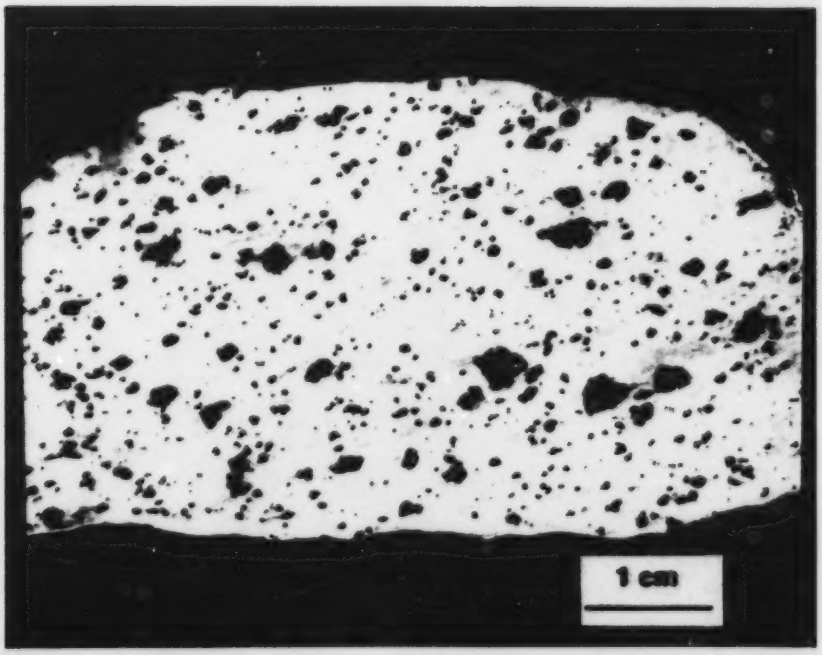

Figure 13: Etched slab, unit 4, showing quartz phenocryst size, abundance and distribution.

Figure 14: Irregular layering trace (highlighted with tape) (20N/156E).

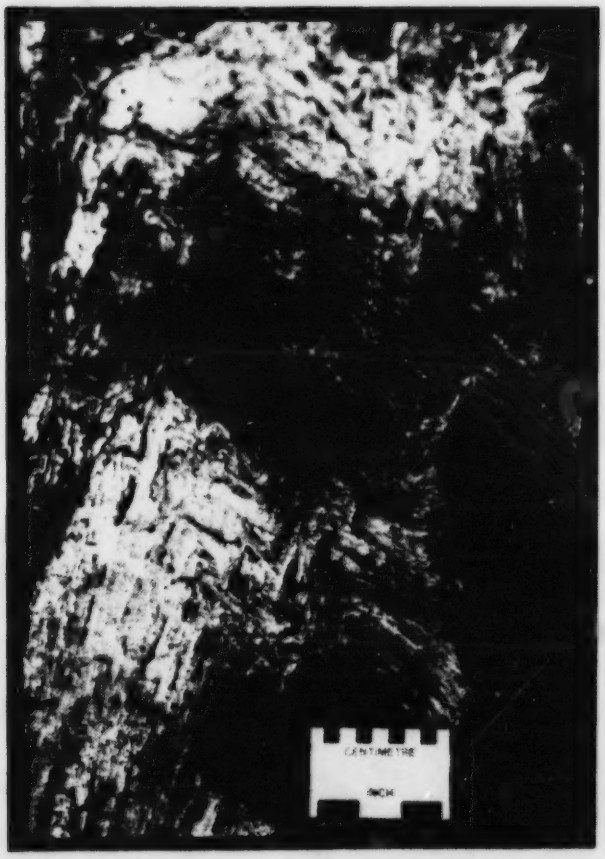

Figure 15: Minor folds (unit 1, 20N/150E).

PLANAR FABRICS

West of Sourdough Bay Fault, contacts between layers have approximately the same orientation. In addition, layers are apparently parallel to primary bed surfaces, but may be transposed to some degree. East of Sourdough Bay Fault, attitudes of layers are quite variable, and although generally undulatory, they are irregular as a result of folding and disruption along cleavage planes (Fig. 3, 14, 15). It is commonly difficult to differentiate beds from transposed beds or structurally derived layers; it is presumed that most layers approximate the orientation of beds.

The earliest recognized foliation (S_1) is approximately parallel to layer surfaces. This penetrative fabric is defined by the alignment of micaceous minerals, and rarely, by quartz phenocrysts in tuffaceous layers and fragments (Fig. 3).

In several parts of the area, most notably southwest of Leo Lake, a strong pervasive cleavage (S_2) is developed in massive and fragmental rhyolitic rocks, as well as folded schistose rocks (Fig. 3). In addition, rock fragments are commonly elongated within the S_2 plane. In the massive rhyolitic rocks, the mm- to cm-spaced S_2 fabric gives the rock a pseudo-conglomeratic appearance. Centimetre-size, lenticular to ovoid chlorite ± sericite ± pyrite domains were observed along S_2 surfaces in drill core. Lenses of vuggy crystalline quartz are also parallel to S_2 in trenches in the northern part of the area. S_2 crosscuts S_1 at many locations.

A fracture cleavage (S_3) is observed in the eastern part of the map area, in parts of units 1, 3 and 4 (Fig. 3). Massive and fragmental rhyolitic rocks with well developed S_3 are characterized by very fine grained, brownish to light-green, recessively weathered chloritic bands that are ≤ 5 mm wide and spaced 2 to 10 cm apart (Fig. 16). These bands may be straight, curved or folded (Fig. 17); evidence of movement along S_3 was not observed.

FOLDS

Minor folds with axial planes that are parallel to the direction of penetrative foliation (S_1) were not observed within the map area. Although S_1 is at a low angle to beds/layers in the area west and northwest of Leo Lake, there are no repetitions of lithologic units that positively identify a major F_1 closure. A plot of poles to beds/layers indicate that beds/layers have apparently been folded about an axial plane oriented approximately 300° with a near vertical dip (Fig. 18). Attitudes of S_1 are variable throughout the map area. A plot of poles to foliation within rock fragments is generally coincident with the attitudes of beds/layers (Fig. 19). No F_2 minor folds were identified in outcrop.

Minor folds that deform S_2 strike 025° to 040°, dip steeply east, and plunge 70°S. These folds were observed in trenches southwest of Leo Lake (e.g., trench 4, Fig. 20). A plot of S_2 poles indicates that S_2 has apparently been rotated about a plane that trends approximately 040° with a steep easterly dip (Fig. 21). Poles to planes of elongation of rock fragments indicate that they have been rotated about the same fold axis as S_2 (Fig. 22). These coincident constructed axial planes indicate that S_2 has been affected by a major F_3 structure that is parallel to the orientation of the minor folds.

Minor folds that deform both S_2 and S_3 strike approximately 080°, dip steeply south, and plunge steeply east or west (Fig. 15, 20, 23, 24). These folds are symmetric to asymmetric, interlimb angles are generally 70° to 80°, and wavelengths are generally less than one metre. It is apparent from a plot of poles to S_3 that S_3 has been affected by a major F_4 fold with an axial plane oriented 085° with a steep southerly dip (Fig. 25). This constructed axial plane approximates the orientation of measured minor folds and an F_4 axial planar schistosity (Fig. 3).

Crenulations and kink folds are developed in schistose chlorite and sericite. These folds are common in the central part of the map area; exaggerated traces are shown in Figure 3. The axial planes to these crenulation folds are mostly oriented 030° to 040° with steep to near vertical dips. However, where F_4 minor folds are readily discernible in outcrop, some of the crenulation fold axes are parallel to the F_4 axial plane.

Locally, a 040°–azimuth cleavage crosscuts S_3 (e.g., 12N/149+50E). This would indicate a later structural event, but there is insufficient evidence to determine that this is a regional structural feature.

FAULTS

The Sourdough Bay Fault (Kalliokoski, 1948), a major north-northeast-trending fault, extends from Sourdough Bay (Lake Athapapuskow) south of the project area through Flintoba Lake and north to Alberts Lake (Fig. 3). This fault is defined by a prominent topographic lineament, offset stratigraphy, and shear textures observed in outcrop, drill core and thin section. Thin sections show a finely granulated groundmass that swirls around phenocrysts that are brecciated *in situ* and have well developed pressure shadows. Alteration assemblages of chlorite + sericite + epidote + (carbonate) + (pyrite) + Fe-Ti oxide minerals commonly form locally crenulated, subparallel streaks. Shear cleavage is particularly prominent in outcrop at 65N/139+50E. Lithologic units are not directly correlatable across the fault within the map area; unit numbers assigned to rocks west of the fault are tentative.

Small fault blocks have been identified in the centre of the map area near baseline 150N (Fig. 3). The faults are defined by offsets in strata, marked by prominent topographic lineaments, and have apparent right-lateral sense of movement, and appear to have developed sub-parallel to S_2.

Minor shears occur in local discrete zones, generally 10 to 20 cm wide, that are straight to curvilinear (Fig. 26, 27, 28). Their average orientation is 015° to 030° azimuth

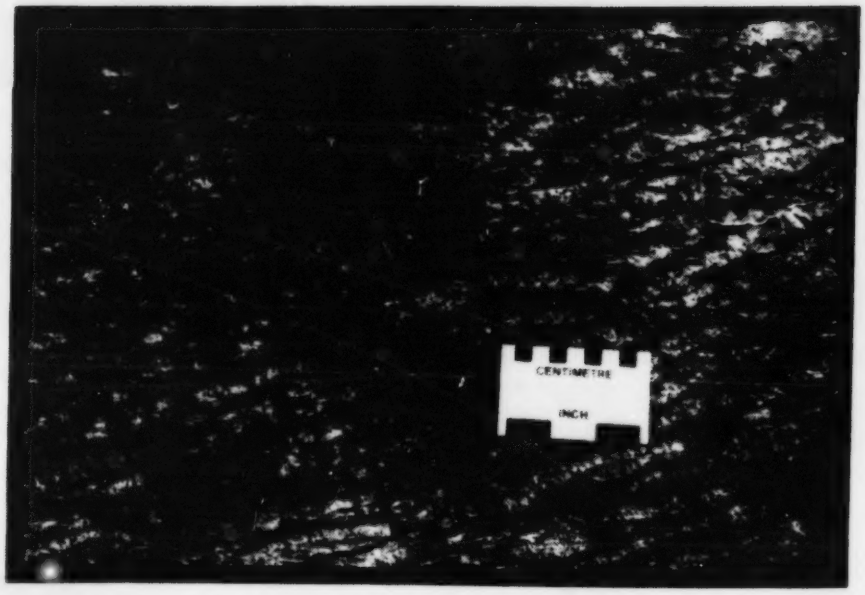

Figure 16: S_3 (unit 1, 20N/157+30E).

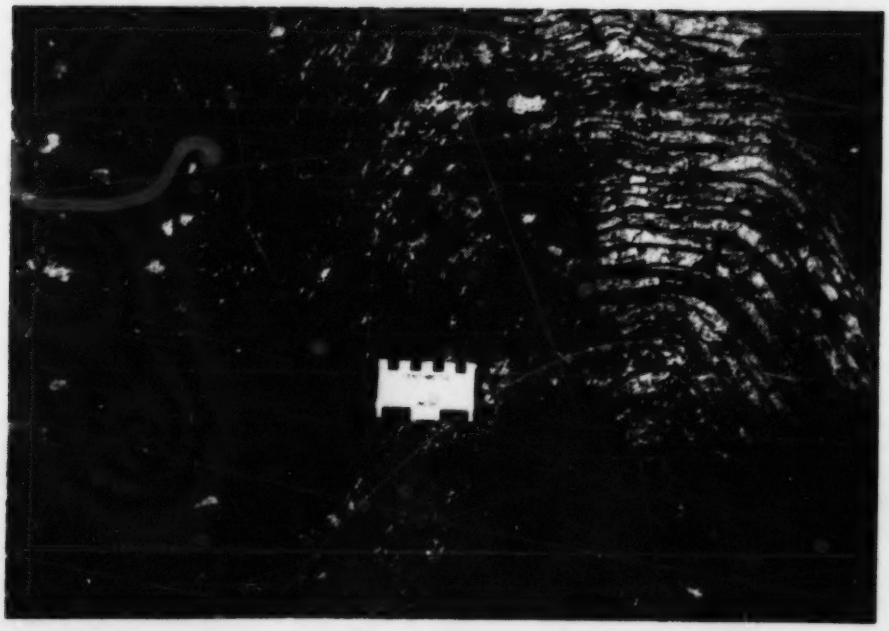

Figure 17: Folded S_3 (unit 1, 22N/162E).

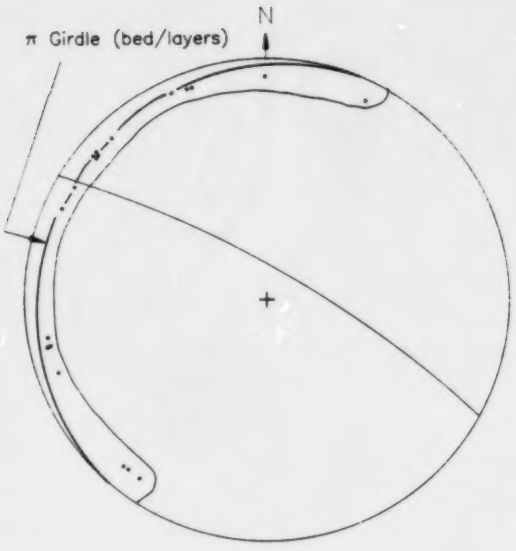

Figure 18: ***Lower hemispheric projection of poles to beds/layers.***

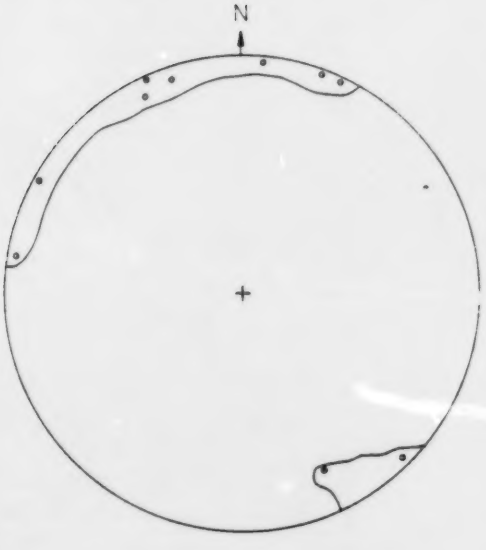

Figure 19: ***Lower hemispheric projection of poles to foliation within rock fragments.***

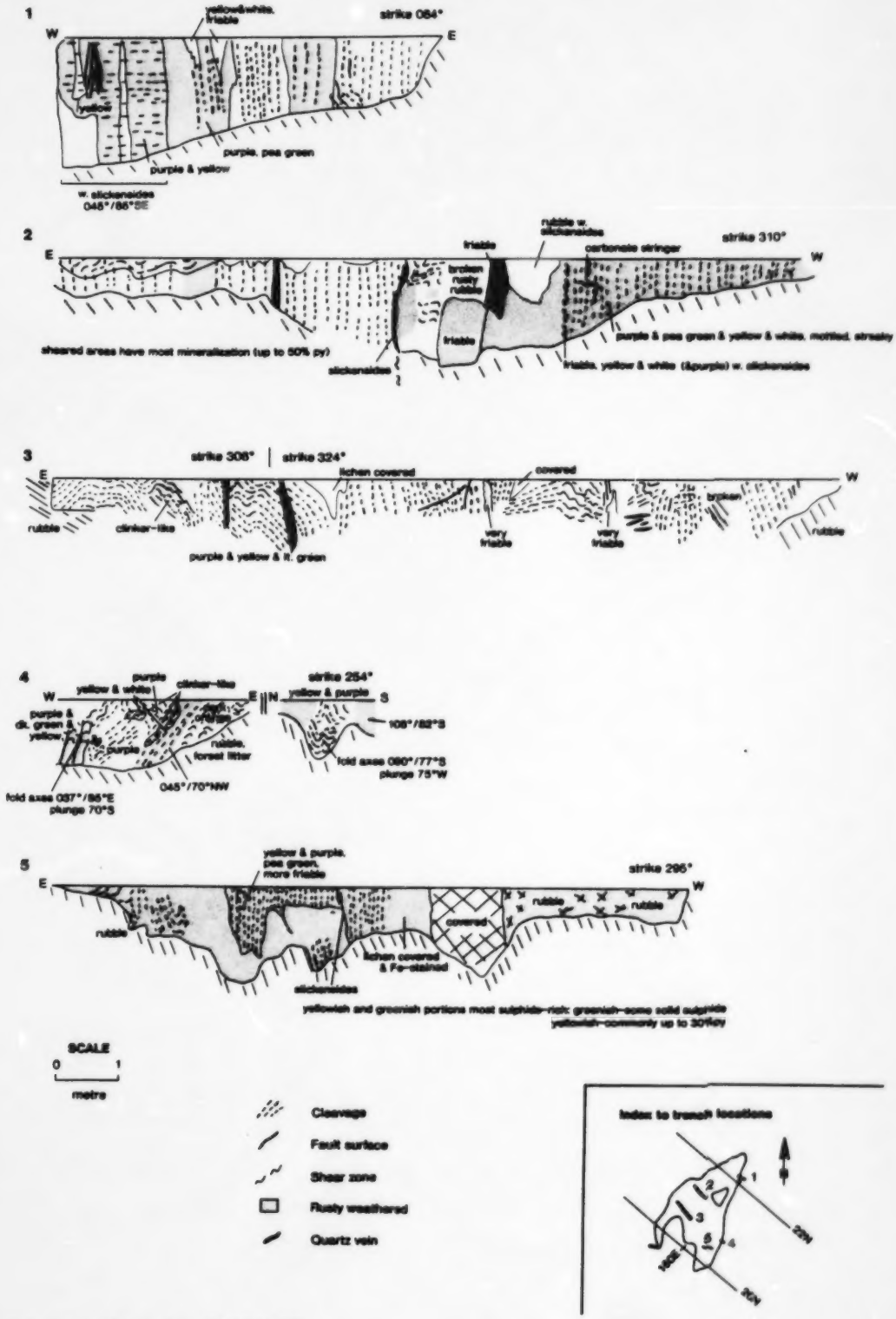

Figure 20: Sketch maps of trenches (20N/160E).

Figure 21: ***Lower hemispheric projection of poles to S_2.***

Figure 22: ***Lower hemispheric projection of poles to planes of elongation of rock fragments.***

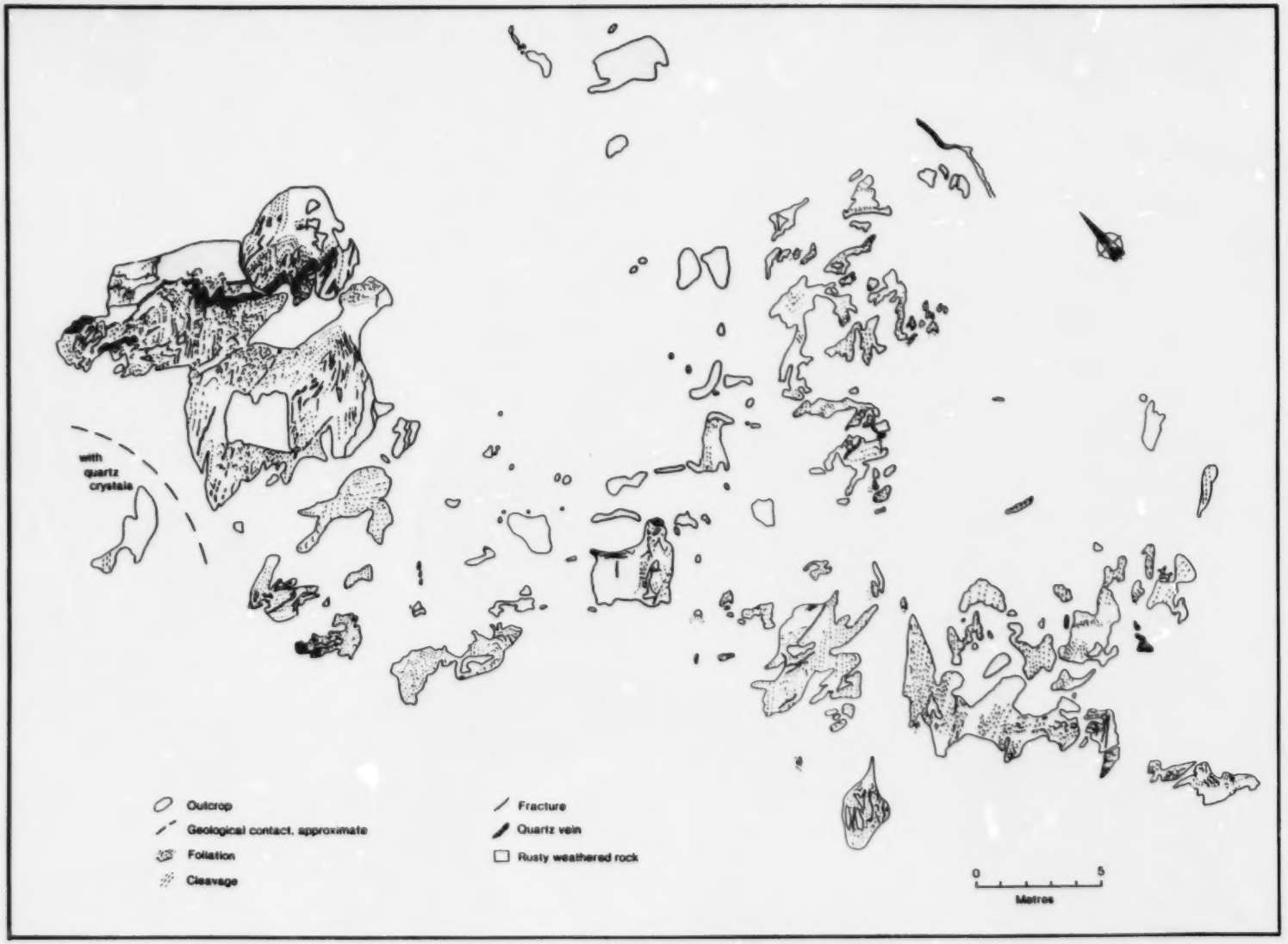

Figure 23: Detailed outcrop map of the area near 10N/148E.

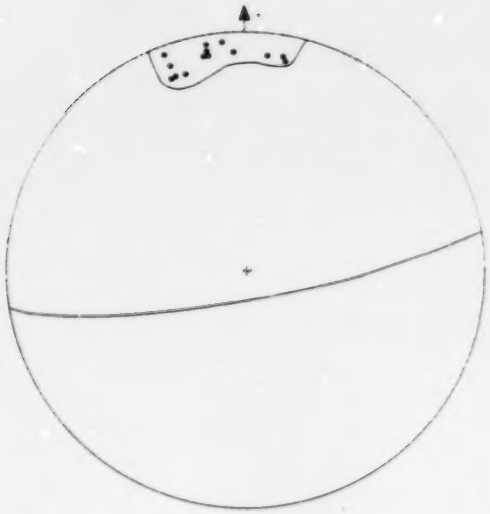

• Poles to axial planes of minor folds

Figure 24: Lower hemispheric projection of poles to minor fold axes.

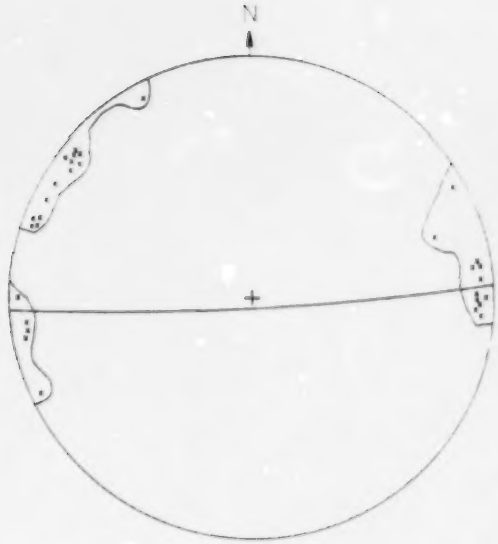

• Poles to S_3

Figure 25: Lower hemispheric projection of poles to S_3.

Figure 26: Representative minor shear zone (unit 2, 12+50N/143E).

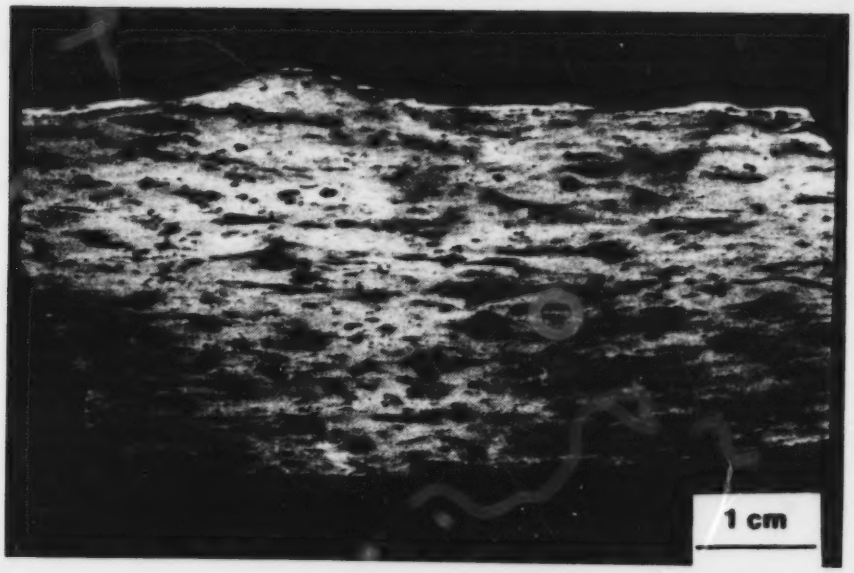

Figure 27: Sheared textures in etched slab, unit 4.

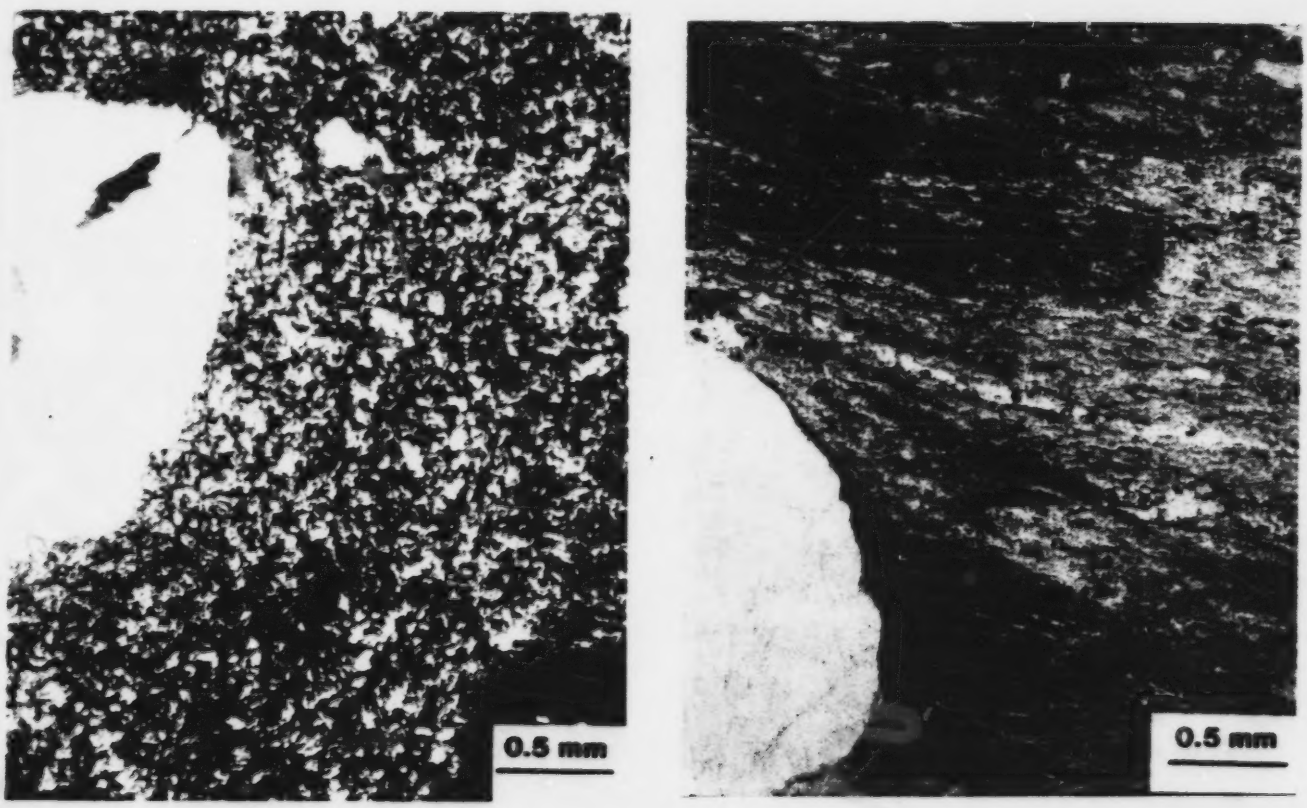

Figure 28: Photomicrograph of (a) nonsheared vs. (b) sheared textures from minor shear zone, unit 4.

with dips that vary from near vertical to steeply east or west (Fig. 29), and are approximately parallel to S_2. Rocks in these zones are mylonitized, and exhibit shear textures in outcrop, drill core and thin section. The shear zones are accompanied locally by irregularly shaped veinlets and pods of quartz-carbonate-(chlorite)-(pyrite). These veinlets are discontinuous, pinch and swell from < 1 mm to 30 cm in width, and are mostly irregularly oriented. However, discrete veinlets that have fairly constant attitudes are more or less parallel to, and commonly form in the axial planes of, F_4 minor folds (Fig. 30).

Slickensides occur on rocks exposed in trenches southwest of Leo Lake. Most slickensides were observed on flyrock, and therefore are not useful in determining sense of movement.

Joint sets are best developed in rocks in the northern part of the map area (Fig. 3); however, no consistent orientation was observed.

INTRUSIONS

Gabbro has been deformed by minor folds and late crenulation folds. The distribution of the gabbro (Bateman and Harrison, 1945) shows that it has been folded about a northeast-trending axis, probably F_3 (Fig. 2). Contact relationships between granodiorite and gabbro have not been observed. The granodiorite has been affected by the Sourdough Bay Fault, but is not obviously folded. Late mafic dykes (see 'Lithologic Units; unit 5') are undeformed.

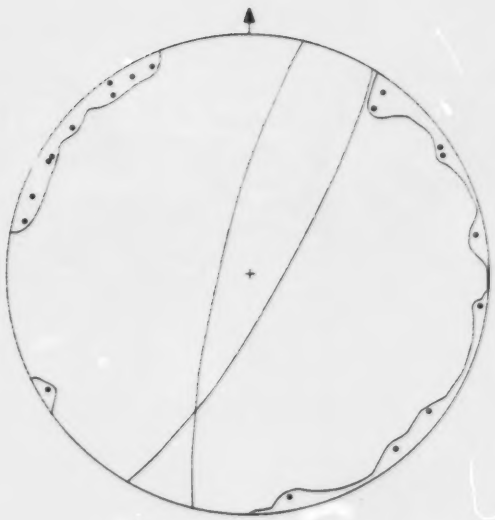

• Poles to shear zone orientations

Figure 29: Lower hemispheric projection of poles to shear zones.

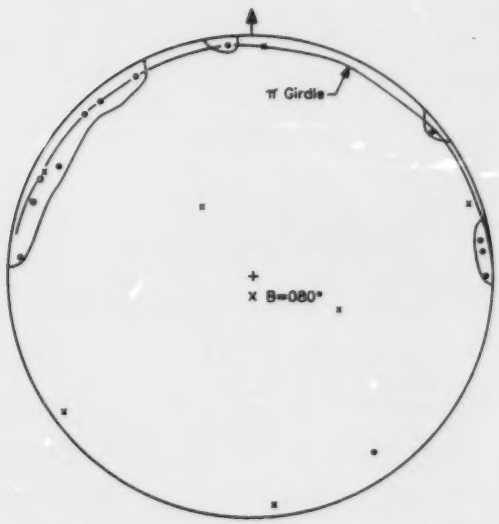

Poles to chlorite or quartz veinlets in felsic rocks:
• quartz; ◦ chlorite; x in gabbro

Figure 30: Lower hemispheric projection of poles to quartz ± chlorite veinlets. The area contains abundant veinlets that have not been plotted because they are irregularly oriented.

Figure 31: Silica network (unit 1, 20+30N/146+50E).

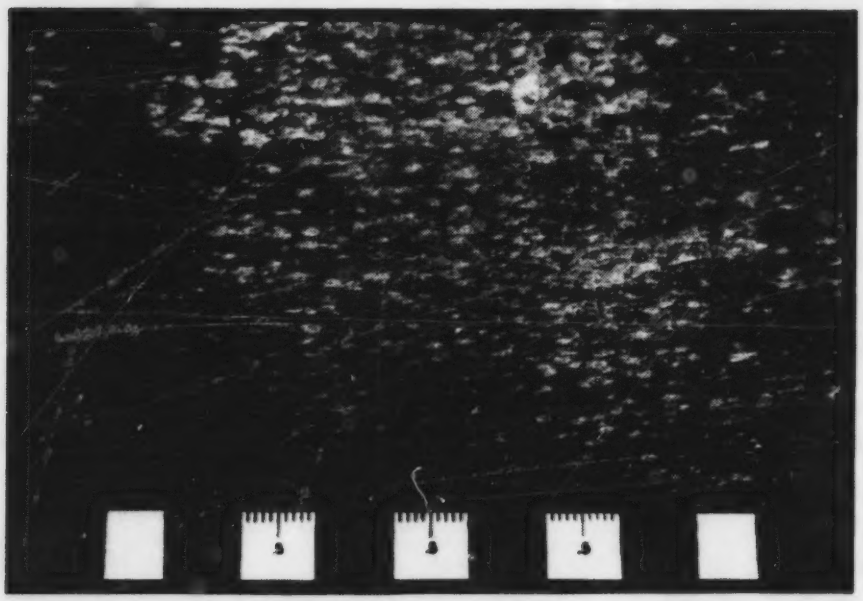

Figure 32: Ovoid 'pseudo-lapilli' in chloritized groundmass (25N/21+40E). Scale bar is graduated in centimetres.

ALTERATION

Rocks in the map area have been extensively chloritized, sericitized, epidotized, pyritized, carbonatized and saussuritized. Fine grained chlorite overprints the rock, forms stringers and elongate patches, and rims phenocrysts. Sericite constitutes elongate streaks along cleavage planes and, to a lesser degree, surrounds lithic fragments and overprints the matrix. Fine grained granular epidote is associated with chlorite and/or sericite. Carbonate is less common, forming small crystals that overprint the matrix and infill microfractures. The matrix, plagioclase phenocrysts and lithic fragments have been lightly to heavily saussuritized, sericitized, chloritized and epidotized. Yellow, grey and white clay occurs in trenches, notably those near the northeast end of Flintoba Lake and those southwest of Leo Lake. Up to 20% sulphide minerals, average 1%, are present in unit 1; these are described in more detail in 'Mineralization'.

Discontinuous mm- to cm-wide quartz veinlets with irregular shape and orientation are common. In addition, quartz occurs as: (1) veinlets parallel to axial planar cleavage or to the hinges of minor folds, (2) tension veins, preferentially oriented approximately east-west and, less prominently, north-south, and (3) irregular pods. Chlorite and/or carbonate also occur as accessory minerals. It has not been determined whether the quartz veinlets are the products of remobilization of silica from the felsic rocks, or result from the addition of silica by alteration; a combination of these two processes is likely. Locally a silica 'network' is superimposed on felsic volcanic rocks from unit 1 (20+30N/146+50E) (Fig. 31).

At 24N/21E, a 60 cm thick bed contains 80% ovoid 'lapilli' that are up to 6 mm, average 3 mm (Fig. 32). The 'lapilli' are not identifiable in thin section; rather, chlorite surrounds ovoid areas of less altered matrix, and the 'lapilli' are probably 'pseudo-fragments' developed by alteration. Lenticular 'pseudo-fragments' of chlorite ± sericite ± pyrite were also identified in drill core.

MINERALIZATION

GENERAL

Felsic volcanic rocks southwest of Leo Lake and on the northeast shore of Flintoba Lake host copper-zinc mineralization collectively known as the Leo Lake occurrence (Fig. 2). Gabbro along the NNE-trending fault zone in the northern part of the map area hosts the Alberts Lake gold deposit (400 000 tonnes grading 7.3 g/t Au) and other smaller vein type gold occurrences (Gale and Eccles, 1988). This section will concentrate on mineralization within the felsic volcanic rocks; Gale and Eccles (1988) provide more information about the gabbro-hosted gold occurrences.

EXPLORATION HISTORY

A summary of the exploration history of the Leo Lake occurrence is presented in Table 1. Locations of drill holes and EM conductors are shown in Figures 33 and 34. In addition to the work shown therein, Granges Inc. has conducted overburden and diamond drilling programs, the results of which are not publicly available.

CHARACTERISTICS OF MINERALIZATION

Chloritic sericitic felsic volcanic rocks of unit 1 host up to 20% disseminated to solid pyrite with minor chalcopyrite and sphalerite. The distribution of sulphide minerals is demonstrated in outcrop by rusty weathered areas; irregular mottled areas are prevalent (Fig. 16, 35), but pervasively rusty weathered areas are also common. Locally, pyrite and chalcopyrite are mobilized and concentrated along fractures in veins up to 10 cm thick, but sulphide minerals are generally not concentrated in or along the margins of quartz veins and veinlets. Angular sulphide fragments and sulphide breccia were noted at one location in unit 1 (Fig. 36, 37).

Units 2 through 4 have minor late euhedral pyrite, generally ≤ 1%, associated with chlorite (± carbonate ± sericite).

Drill holes intersected siliceous, sericitic, chloritic felsic volcanic rocks, including fragmental rocks that range from tuff to breccia, minor chlorite schist and minor porphyry sections (Assessment File 90435, Manitoba Energy and Mines). Sheared sections are commonly noted in drill logs, but mineralization does not appear to be concentrated in or along the margins of these zones. Nonmineralized quartz stringers are common. Minor pyrite is disseminated throughout most of the drill core. Chalcopyrite occurs as rare disseminated grains, blebs and thin stringers associated with pyrite and rarely with quartz-carbonate veinlets. Several "well mineralized" to near solid pyrite (+ chalcopyrite) sections were intersected in drill core; these sections are up to 1.3 m in core length, but average 0.1 m.

The majority of exploration activity has been directed towards two areas of intensely rusty weathered outcrops from unit 1, termed the 'East Zone' and the 'West Zone' by Gale and Eccles (1988) (Fig. 33).

The East Zone consists of several large outcrops near 20N/160E that are intensely rusty weathered, altered and deformed (Fig. 33). These rocks were affected by F_2 folding, and are crosscut by numerous late fractures and shear zones, parallel to the F_1 axis, that concentrate and displace mineralization. Trench maps from the vicinity of 20N/160E demonstrate the nature and distribution of mineralization and alteration (Fig. 20).

In addition to pyrite and chalcopyrite, sphalerite blebs and bands associated with pyrite were noted in drill logs from several of the holes drilled through the East Zone. Native copper associated with pyrite stringers in rhyolite was noted at one location in DDH A-15 (*ibid.*). Figure 34 shows intersections with significant Cu and Zn contents from holes drilled by God's Lake Gold Mines Ltd (Assessment File 90427, Manitoba Energy and Mines).

The West Zone consists of several intensely rusty weathered outcrops and pits near the northeast shore of Flintoba Lake (Fig. 33). Several core samples with approximately 1.00 to 1.50% Cu over 0.1 to 0.2 m core length were noted in drill logs; numerous assays with less than 1.0% Cu were reported. The highest assay was 2.39% Cu and 3.8 g/t Ag over 0.6 m in DDH T115. Drill logs from Assessment File 90435 also report that samples were assayed for Zn and Au, but results were nil.

Drilling by Granges Inc. intersected gold and silver mineralization hosted by narrow, east-west striking, sigmoidal quartz tension veins north of Flintoba Lake (Fig. 33). Some of these veins contain pyrite, tetrahedrite(?), chalcopyrite, chlorite(?), visible gold, and possible native silver (Granges Inc., pers. comm., 1988).

Table 1

Summary of exploration history of the Leo Lake occurrence (after Mineral Inventory Card 63K/13SE Cu10; Gale and Eccles, 1988; and records of the Mining Recording Office, Manitoba Energy and Mines Minerals Division)

Year	Activity
1920	Staked as Cap claim by E. Brydges
1920-1927	Surface work, sporadic
1927	Partial interest assigned to W. Baker and E. Patton
1928	Optioned to Flintoba Mines Limited; trenching, at least one drill hole (150 m long)
1931	Partial interest assigned to W. Govan
1937	Cap claim cancelled
1938	Cap claim staked by O. Hilton, assigned to W. Govan
1939-42	Surface work
1944	Cap claim cancelled
1944	Wally 16 claim staked by G.N. Moore, assigned to Consolidated Mining and Smelting Company Limited
1945	Interest assigned to F.G. Whitaker
1947	Wally 16 claim cancelled
1947	J.S. 7 claim staked by J.J. Johnson
1948	Interest assigned to H.C. Stevens
1948-50	Surface work
1950	Optioned to Hudson Bay Exploration and Development Company Limited
1951	Geological mapping, 7 diamond drill holes
1953	Option abandoned
1955	God's Lake Gold Mines Limited drilled 17 holes
1956	Interest assigned to B.N. Apple
1958	Trenching
1962	J.S. 7 claim cancelled
1962	Mark 2 claim staked by B.P. Poulin
1963-65	Surface work
1966	Mark 2 claim cancelled
1967	Flin 2 claim staked by J. Murray, assigned to Guggenheim Exploration Inc.
1967	Horizontal and vertical loop EM surveys; one diamond drill hole
1974	Flin 2 claim cancelled
1974	C.B. 4256 claim and Mud 3 fraction staked by A.J. O'Donnell
1976	Holder's name changed to A.L. Parres, then to Pinebay Mines Limited
1978	C.B. 4256 cancelled
1979	ALP 3 claim staked by Pinebay Mines Ltd.
1990	Interest transferred to Granges Inc.
1979	Geo 1 and Geo 2 claims staked by A.L. Parres Ltd.
1981	Holder's name changed to SMD Mining Co. Ltd.
1983	Interest transferred to A.L. Parres Ltd.
1990	Interest transferred to Granges Inc.

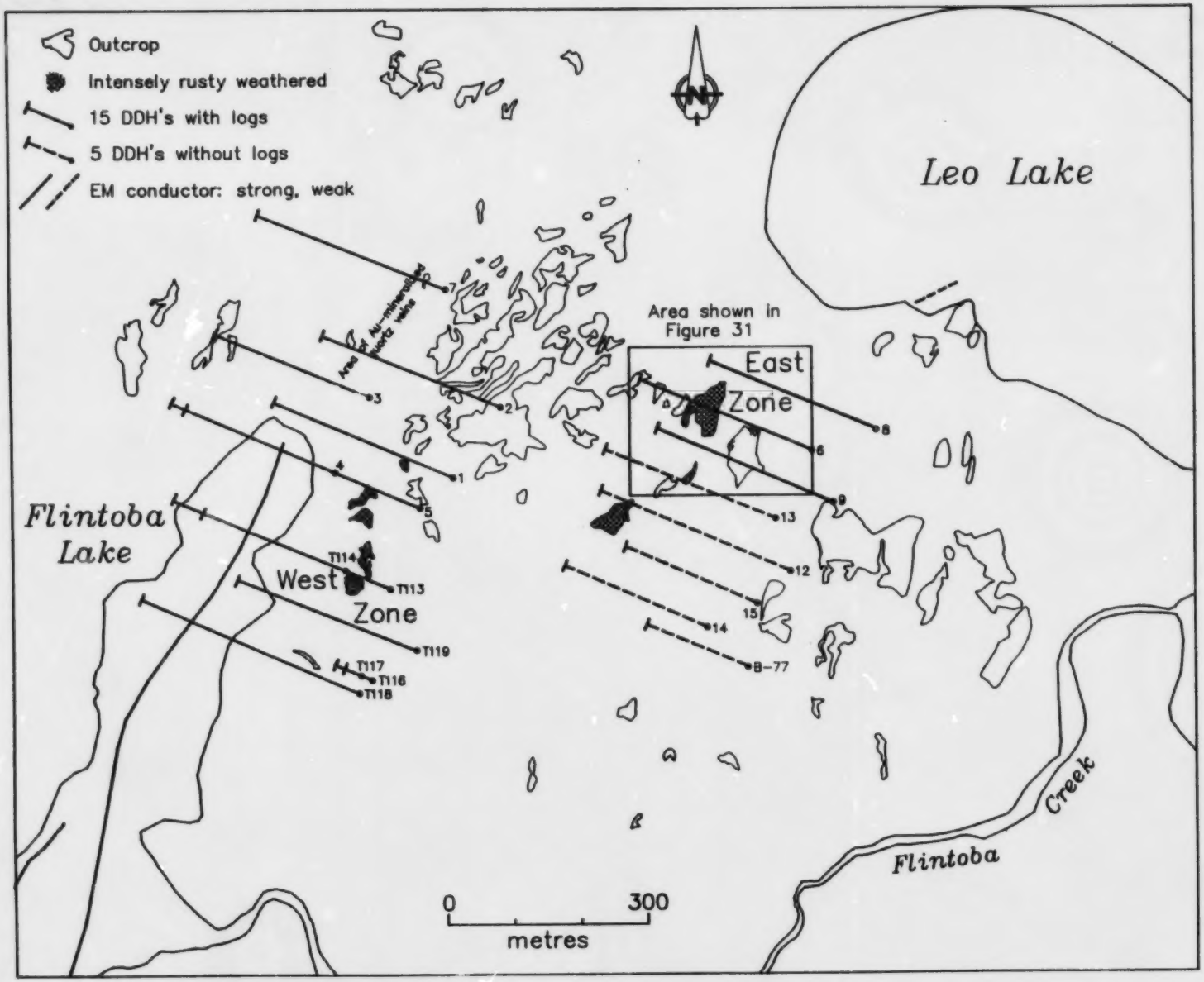

Figure 33: Location of diamond drill holes and electromagnetic conductors (modified from Gale and Eccles, 1988).

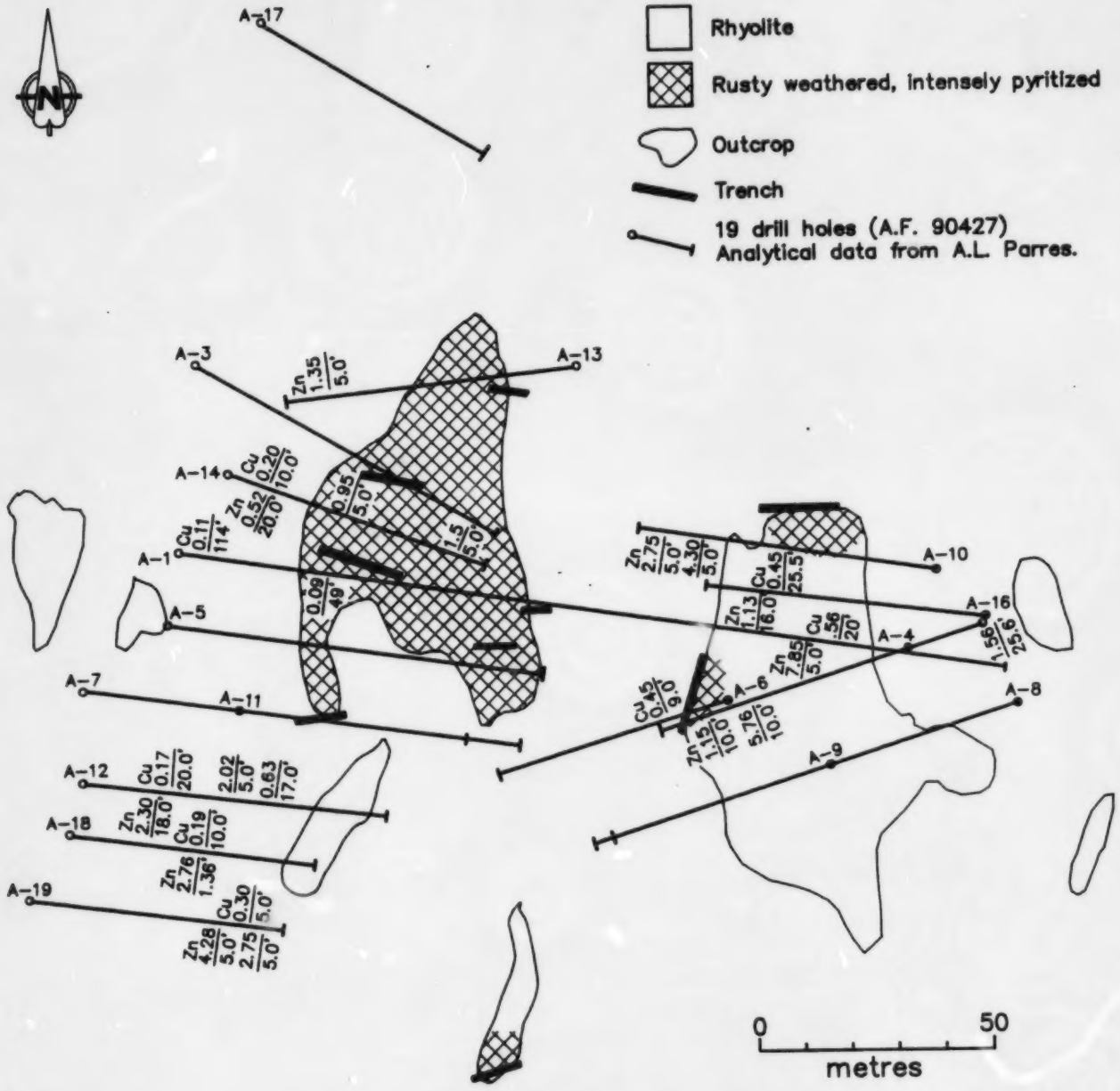

Figure 34: Location of holes drilled on the East Zone by God's Lake Mines Ltd. (Gale and Eccles, 1988). See Figure 33 for location of area.

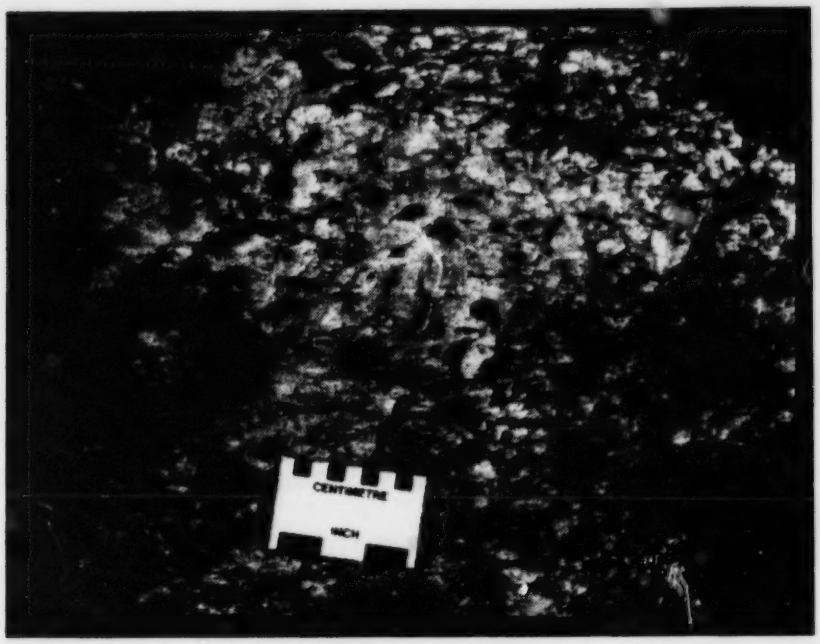

Figure 35: Lapilli tuff with irregular rusty weathered areas (unit 1).

Figure 36: Angular sulphide clast in quartz-phenocryst-poor rhyolitic lapilli tuff (unit 1, 20N/147+20E).

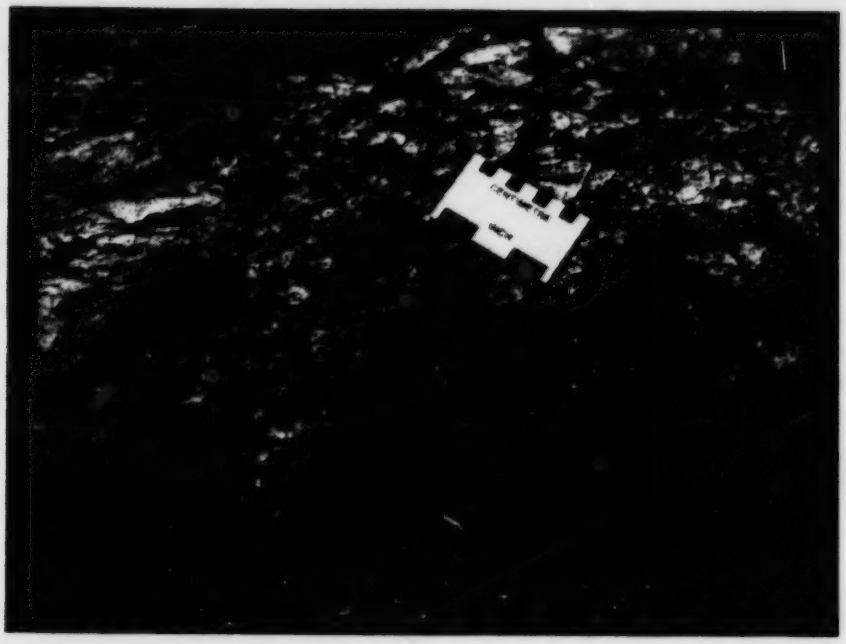

Figure 37: Sulphide breccia (unit 1, 20N/147+20E).

SILICATE WHOLE-ROCK ANALYSIS

Introduction

Felsic volcanic rocks were sampled in order to determine typical compositions and to check for systematic compositional differences due to alteration. The samples were also analyzed for copper and zinc concentrations.

Sample Collection, Preparation and Analytical Methods

Individual samples consisted of 1 to 3 kg of 2 to 5 cm-size rock chips collected with sledge hammers and visually screened to avoid obviously weathered or mineralized material. The 'M-' samples were collected in 1980 as part of a sampling program that covered most of the Baker Patton felsic complex (G.H. Gale, unpublished data). The 'M-' samples were located on 1:5 000 airphotos at the time they were collected; these locations have been transferred to the grid map with reasonable success, but their locations are not accurate. Additional samples ('LEO-' prefixes) were collected during the course of this mapping program to provide additional coverage where warranted. Sample locations are shown on Figure 38 (in pocket).

Samples were crushed into 6 mm fragments and ground to -200 mesh in a Spex shatterbox using a tungsten carbide dish and puck. SiO_2, Al_2O_3, TiO_2, P_2O_5 and FeO^T were determined by colorimetry, and CaO, MgO, Na_2O, K_2O, MnO, Cu and Zn were measured by atomic absorption spectrometry after a HF-$HClO_4$ total extraction. CO_2 was measured in an induction furnace. LOI was determined by the Penfield Method. All analyses were performed at Manitoba Energy and Mines Analytical Laboratory, Winnipeg.

Results

Major element analyses are presented in Appendix I; Cu and Zn analyses are presented in Appendix II. Tables 2 through 6 summarize the descriptive statistics for analyses for all samples in the data set, as well as for individual units. Table 7 presents a Spearman nonparametric correlation coefficient matrix for the data.

Compositions range from dacitic to rhyolitic with a mean of 71.9% SiO_2 and a range from 63.8% to 81.0% (Table 2). The lowest values (i.e., < 65% SiO_2) are from rocks in unit 2. However, samples from unit 2 do not have uniformly lower SiO_2 contents than other units; the more heterolithic character of the fragments in unit 2 than other units may be a factor in this range of SiO_2 contents. The highest SiO_2 contents are from units 1 and 3, but there is a fairly wide range of SiO_2 contents in these units as well (67.5 to 81.0% SiO_2 in unit 1; 66.0 to 80.1% SiO_2 in unit 3). Le Maitre (1976) gives an average SiO_2 content of 74.0% with a standard deviation of 3.5 for rhyolite. Felsic rocks throughout the Baker Patton felsic complex have a mean of 71.4% SiO_2 with a standard deviation of 4.0 (G. Gale, unpublished data). The highest SiO_2 contents from this map area are substantially higher, and suggest that silicification may have affected these rocks. Field evidence of silicification was presented in 'Alteration'.

Al_2O_3 contents range from 8.5% to 14.7% with a mean of 11.8% (Table 2). There is a strong statistical correlation with SiO_2 (Table 7), as would be expected from felsic volcanic rocks with their abundance of aluminosilicate minerals.

FeO^T contents range from 0.3 to 8.9% with a mean of 4.6% (Table 2). These are fairly high for felsic volcanic rocks, and suggest enrichment by pyritization and chloritization. FeO^T correlates strongly with P_2O_5 and with MnO, which reflects the Fe/Mn substitution mechanism. There is a significant negative correlation with Na_2O and SiO_2 (Table 7), which suggests a positive correlation between pyritization and sodium depletion, and a negative correlation between pyritization and silicification.

CaO contents range from 0.00 to 2.45% with a mean of 0.6% (Table 2). These results indicate that the rocks have been significantly depleted in calcium.

MgO contents range from 0.42% to 5.38% with a mean of 2.99% (Table 2, Fig. 39). Samples with high MgO contents correlate positively with visual observations of abundant chlorite in outcrop and in thin section: the high magnesium content probably reflects chloritization.

Na_2O contents range from 0.14% to 5.73% with a mean of 1.95% (Table 2). All units contain some rocks that are significantly depleted in sodium, as well as some rocks that are not sodium depleted, however a contour map of Na_2O contents shows a broad area of sodium depletion in the centre of the sampled area (Fig. 40). There is strong positive correlation between Na_2O and CaO contents and negative correlation between Na_2O and MgO (Table 7, Fig. 39, 40), which reflect the coincidence of sodium- and calcium depletion and chloritization.

K_2O contents range from 0.30 to 3.76% with a mean of 1.60% (Table 2), indicating that rocks are potassium depleted. However, sericite is a prominent alteration mineral (see 'Alteration'). A significant negative correlation between K_2O and Na_2O (Table 7) may reflect coexistent sericitization and sodium depletion. There is no systematic variation in (Na_2O + K_2O). K_2O contents are notably higher in rocks from the southern part of unit 3 than from the northern part of the unit (ranges of 2.09 to 3.76% K_2O and 0.34 to 2.60% K_2O, means of 3.02% K_2O and 1.25% K_2O, respectively; Fig. 41).

LOI contents have a range of 1.5 to 5.3% and a mean of 3.8% (Table 2). These high contents have a strong positive correlation with MgO (Table 7, Fig. 42), probably reflecting chloritization. A significant negative correlation between SiO_2 and LOI may suggest an inverse relationship between silicification and chloritization (Table 7).

TiO_2 contents range from 0.07% to 0.42% with a mean of 0.29%; MnO contents have a range of 0.01 to 0.21% and a mean of 0.06%; P_2O_5 contents average 0.08% and range from 0.04% to 0.19% (Table 2). These analyses are characteristic for felsic volcanic rocks (Le Maitre, 1976).

Table 2: Summary of descriptive statistics for felsic volcanic rocks, Leo Lake area

	SiO_2	Al_2O_3	FeO^T	CaO	MgO	Na_2O	K_2O	TiO_2	P_2O_5	MnO	LOI
No. of cases	65	65	65	65	65	65	65	65	65	65	65
Minimum	63.8	8.5	0.29	0.00	0.42	0.14	0.30	0.07	0.04	0.01	1.5
Maximum	81.0	14.7	8.88	2.45	5.38	5.73	3.76	0.42	0.19	0.21	5.3
Range	17.2	6.2	8.59	2.45	4.96	5.59	3.46	0.35	0.15	0.20	3.8
Mean	71.9	11.8	4.63	0.64	2.99	1.95	1.60	0.29	0.08	0.06	3.2
Std. Dev.	3.7	1.3	1.87	0.68	1.20	1.71	0.77	0.07	0.03	0.04	0.8
Skewness	0.2	0.2	-0.42	1.26	-0.07	0.52	0.70	0.77	1.74	1.62	-0.1
Kurtosis	-0.1	-0.5	-0.01	0.45	-0.74	-1.08	0.19	1.43	4.43	3.38	-0.1

Table 3: Summary of descriptive statistics for unit 1, Leo Lake area

	SiO_2	Al_2O_3	FeO^T	CaO	MgO	Na_2O	K_2O	TiO_2	P_2O_5	MnO	LOI
No. of cases	28	28	28	28	28	28	28	28	28	28	28
Minimum	67.5	9.4	0.68	0.00	1.06	0.21	0.80	0.20	0.05	0.01	1.70
Maximum	81.0	13.5	8.12	1.18	5.27	4.19	2.62	0.40	0.12	0.21	5.10
Range	13.5	4.1	7.44	1.18	4.21	3.98	1.82	0.20	0.07	0.20	3.40
Mean	72.7	11.3	4.76	0.31	3.39	1.22	1.62	0.29	0.08	0.07	3.38
Std. Dev.	2.9	1.0	1.70	0.30	0.97	1.36	0.54	0.05	0.02	0.05	0.65
Skewness	0.6	0.6	-0.52	1.25	-0.49	1.16	0.15	-0.41	0.31	1.17	-0.40
Kurtosis	1.0	0.3	0.17	0.94	-0.14	-0.19	-1.00	0.70	-0.01	0.98	1.62

Table 4: Summary of descriptive statistics for unit 2, Leo Lake area

	SiO_2	Al_2O_3	FeO^T	CaO	MgO	Na_2O	K_2O	TiO_2	P_2O_5	MnO	LOI
No. of cases	16	16	16	16	16	16	16	16	16	16	16
Minimum	63.8	10.5	0.59	0.01	0.42	0.28	0.33	0.07	0.04	0.02	1.80
Maximum	78.4	14.7	5.62	2.45	5.38	5.73	3.62	0.40	0.07	0.07	5.30
Range	14.6	4.2	5.03	2.44	4.96	5.45	3.29	0.33	0.03	0.05	3.50
Mean	70.6	12.8	3.55	1.01	3.15	2.74	1.64	0.27	0.06	0.04	3.49
Std. Dev.	4.2	1.5	1.71	0.81	1.50	1.86	0.87	0.01	0.01	0.02	0.84
Skewness	0.1	-0.5	-0.45	0.56	-0.21	0.12	0.71	-0.97	-0.70	0.35	-0.04
Kurtosis	-0.9	-1.2	-1.23	-1.05	-1.05	-1.25	-0.18	0.16	-0.59	-1.07	0.20

Table 5: Summary of descriptive statistics for unit 3, Leo Lake area

	SiO_2	Al_2O_3	FeO^T	CaO	MgO	Na_2O	K_2O	TiO_2	P_2O_5	MnO	LOI
No. of cases	11	11	11	11	11	11	11	11	11	11	11
Minimum	66.0	10.3	0.29	0.08	0.42	0.29	0.34	0.25	0.07	0.01	1.5
Maximum	80.1	14.2	7.68	2.25	3.08	4.76	3.76	0.40	0.19	0.13	4.8
Range	14.1	3.9	7.39	2.17	2.66	4.47	3.42	0.15	0.12	0.12	3.3
Mean	60.6	12.0	5.26	1.16	2.07	2.37	1.89	0.34	0.11	0.06	3.0
Std. Dev.	4.1	1.1	2.15	0.75	0.76	1.44	1.14	0.06	0.04	0.03	1.0
Skewness	1.1	0.3	-1.03	0.00	-0.89	-0.09	0.19	-0.03	0.81	0.55	0.4
Kurtosis	0.6	-0.3	0.54	1.37	0.10	-1.02	-1.18	-1.56	0.18	0.27	-0.7

Table 6: Summary of descriptive statistics for unit 4, Leo Lake area

	SiO_2	Al_2O_3	FeO^T	CaO	MgO	Na_2O	K_2O	TiO_2	P_2O_5	MnO	LOI
No. of cases	10	10	10	10	10	10	10	10	10	10	10
Minimum	68.3	8.5	1.88	0.03	1.32	0.14	0.30	0.20	0.05	0.02	1.60
Maximum	78.9	13.3	8.88	1.79	4.62	4.86	2.50	0.42	0.12	0.09	3.80
Range	10.6	4.9	7.00	1.76	3.30	4.72	2.20	0.22	0.07	0.07	2.20
Mean	73.2	11.5	5.28	0.39	2.64	2.28	1.19	0.30	0.08	0.05	2.65
Std. Dev.	3.4	1.4	1.73	0.53	1.17	2.02	0.58	0.07	0.02	0.02	0.74
Skewness	0.3	-0.8	0.15	2.10	0.57	0.10	0.92	-0.00	0.78	0.52	0.13
Kurtosis	-0.7	0.2	1.13	3.24	-0.97	-1.65	1.08	-0.90	0.44	-0.67	-1.29

Table 7: Spearman correlation coefficient matrix for felsic volcanic rocks, Leo Lake area (N=65)

	SiO_2	Al_2O_3	FeO^T	CaO	MgO	Na_2O	K_2O	TiO_2	P_2O_5	MnO	LOI	Cu	Zn
SiO_2	1.00												
Al_2O_3	-0.73	1.00											
FeO^T	-0.50	0.10	1.00										
CaO	-0.55	0.50	-0.11	1.00									
MgO	-0.42	-0.20	0.37	-0.08	1.00								
Na_2O	-0.23	0.43	-0.34	0.63	-0.50	1.00							
K_2O	0.15	-0.14	-0.20	0.24	0.10	-0.46	1.00						
TiO_2	-0.53	0.47	0.42	0.32	0.01	0.16	-0.15	1.00					
P_2O_5	-0.34	0.08	0.46	0.11	-0.10	-0.01	-0.10	0.62	1.00				
MnO	-0.44	0.15	0.60	0.11	0.39	-0.12	-0.11	0.28	0.25	1.00			
LOI	-0.62	0.28	0.38	0.30	0.75	-0.30	0.20	0.12	0.01	0.36	1.00		
Cu	-0.38	0.24	0.32	0.33	0.14	0.12	-0.05	0.22	0.16	0.33	0.28	1.00	
Zn	-0.38	0.18	0.31	0.04	0.46	-0.23	0.33	0.11	0.09	0.66	0.50	0.42	1.00

r=0.29 (denotes statistical significance at 99% level of confidence)

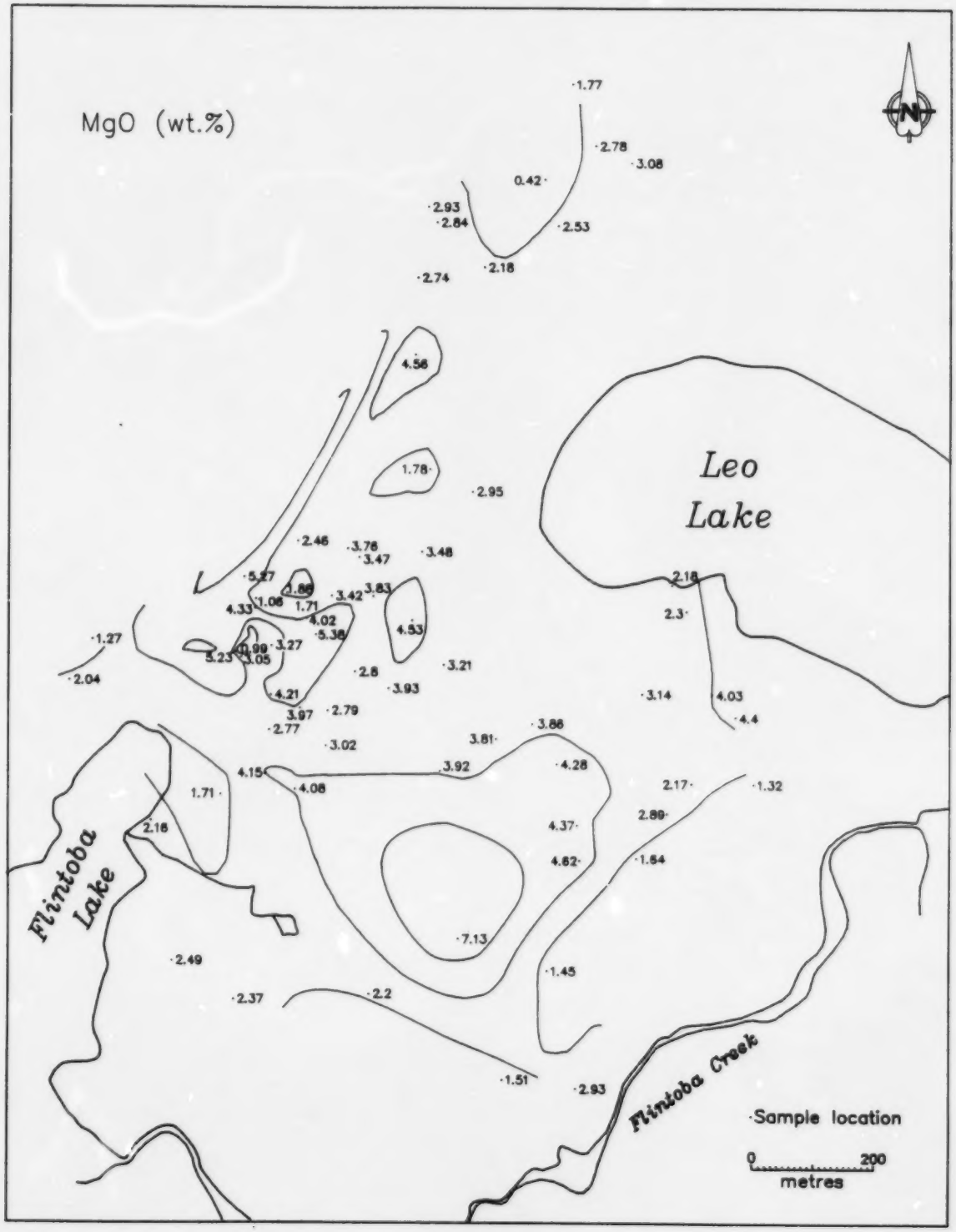

Figure 39: Contour map of MgO (wt. %) distribution. Contour interval = 1%.

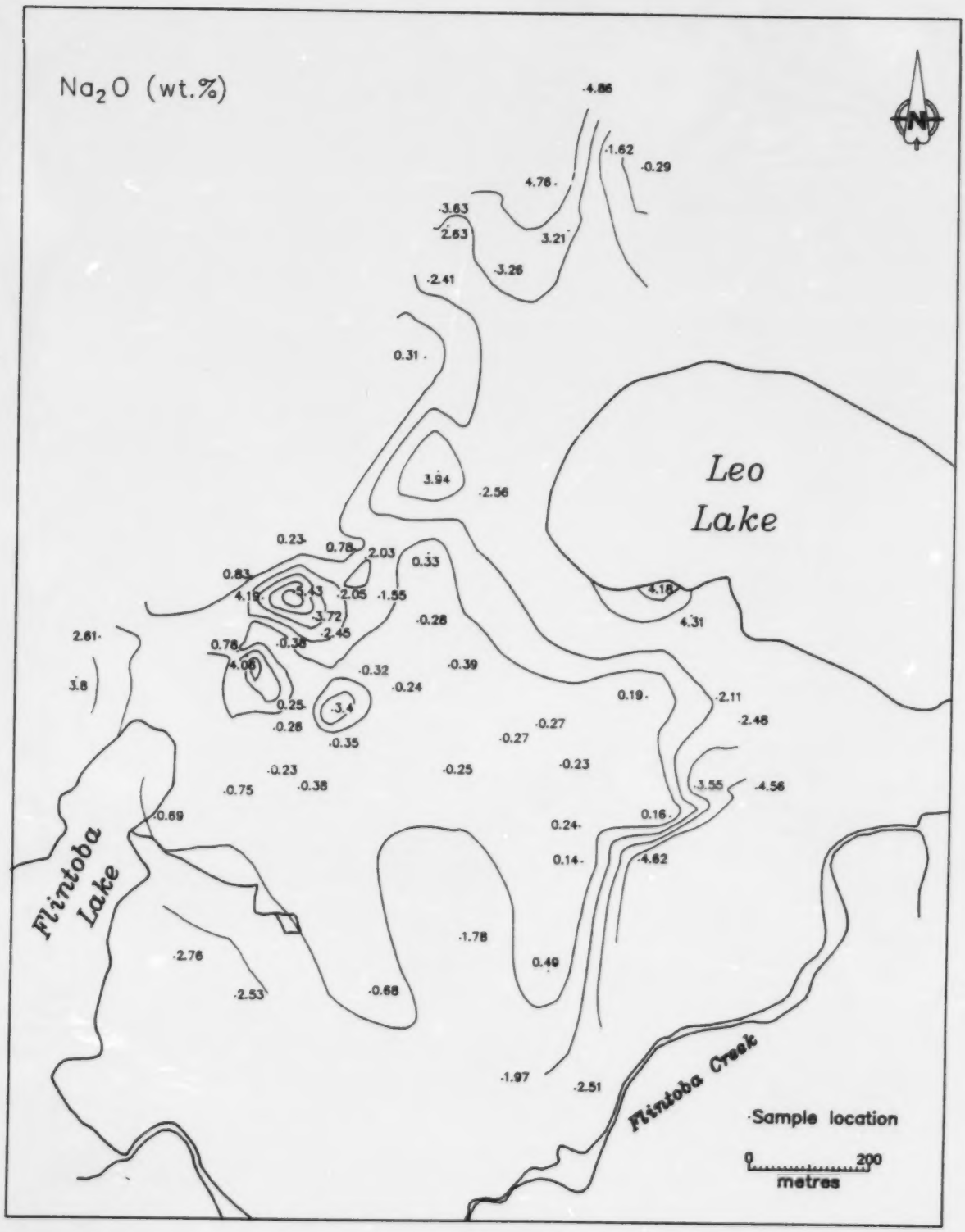

Figure 40: Contour map of Na_2O (wt. %) distribution. Contour interval = 1%.

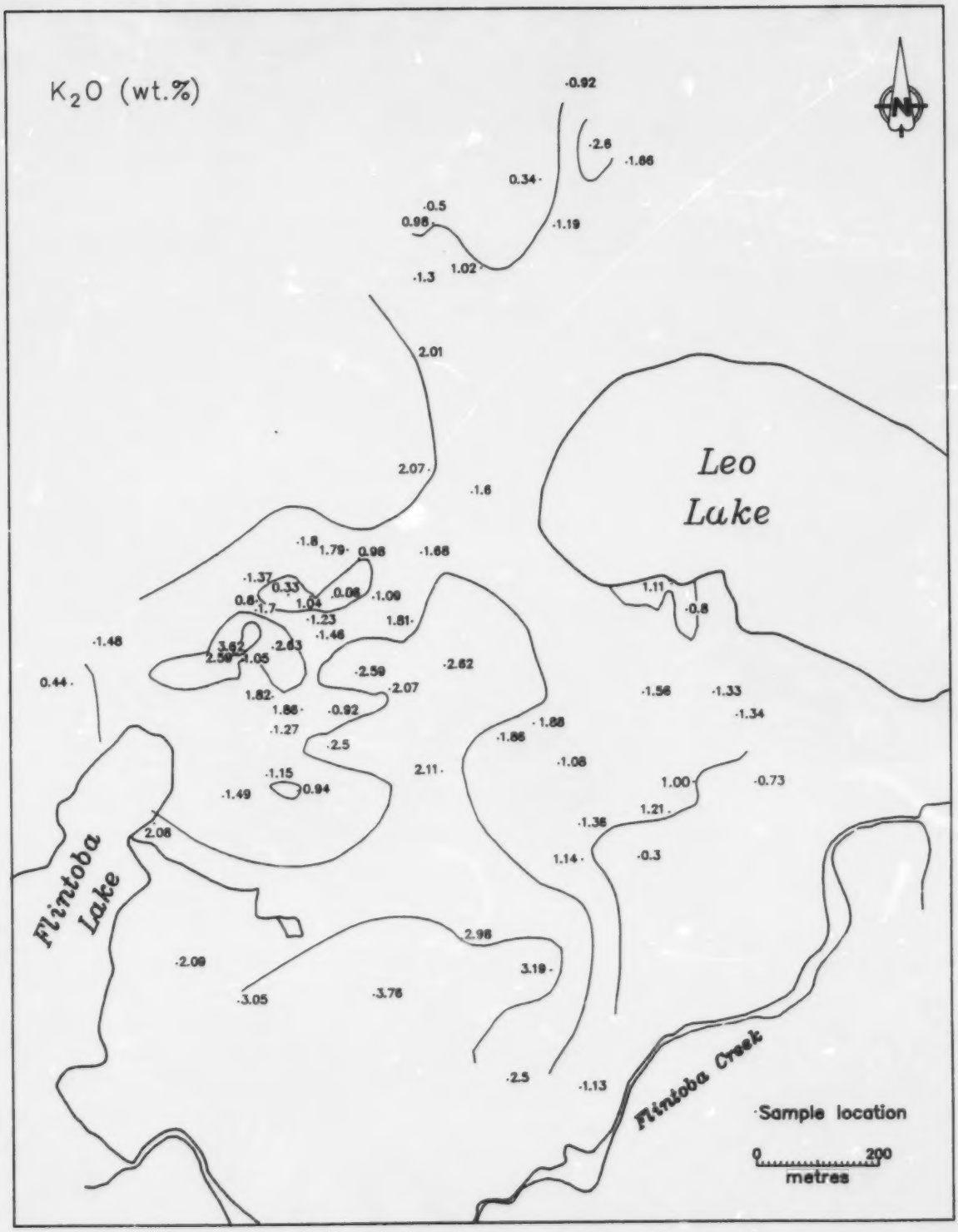

Figure 41: Contour map of K_2O (wt. %) distribution. Contour interval = 1%.

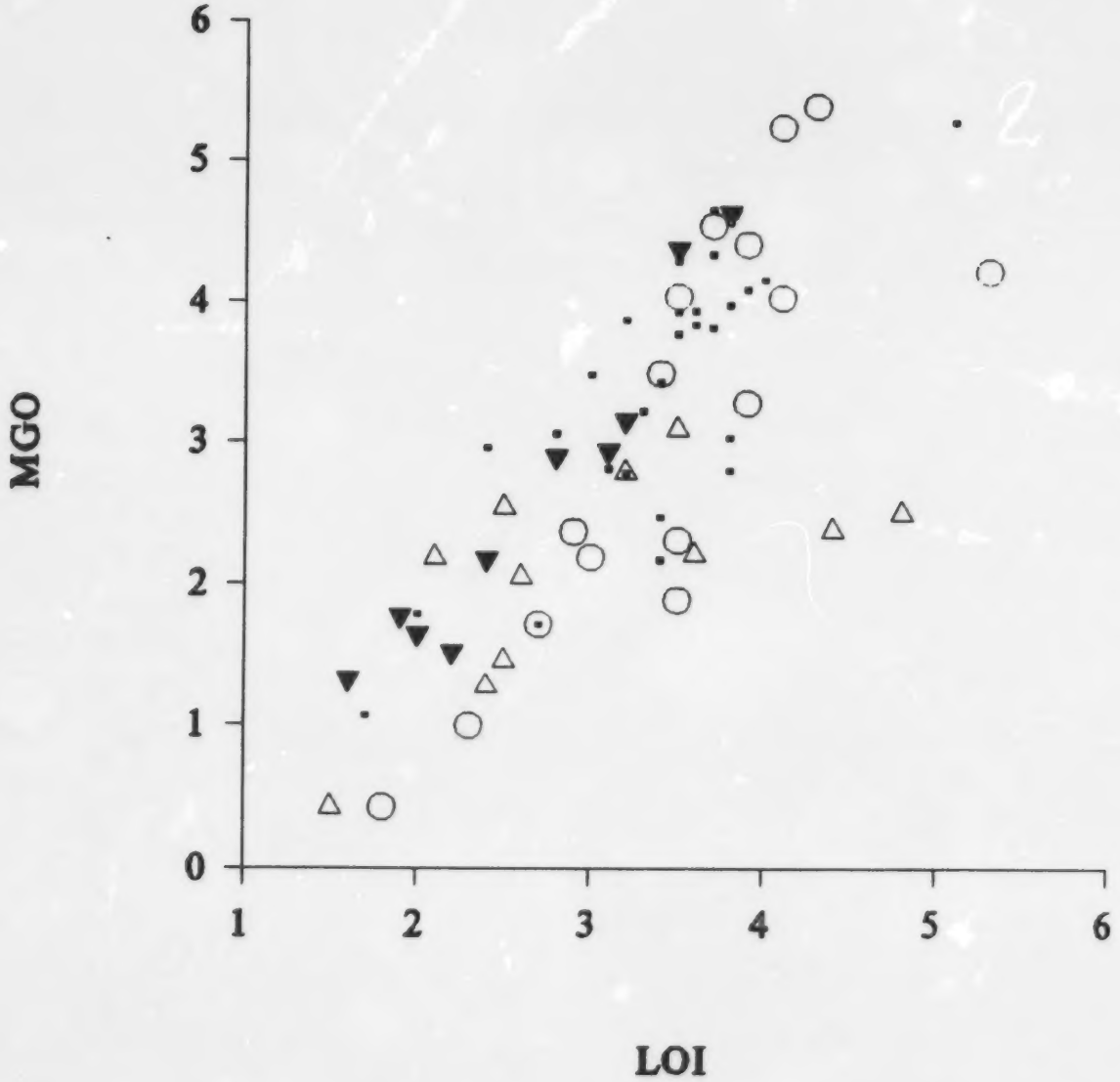

Figure 42: MgO (wt. %) vs. LOI (wt. %). Symbols represent lithologic units: (1) small boxes, (2) open circles, (3) upright triangles, (4) inverted triangles.

Copper and zinc contents are variable, with ranges of 5 to 410 ppm and 2 to 600 ppm, respectively (Fig. 43, 44). High zinc contents (> 100 ppm) are restricted to samples from units 1 and 3. Copper distribution appears to be more erratic; copper correlates weakly with zinc, but does not correlate with concentrations of other elements (Table 7). There is a strong positive correlation between MnO and Zn, reflecting the mineralogical Mn/Zn substitutional mechanism. A significant positive correlation between Zn and MgO and LOI (Table 7), and poor negative correlations between SiO_2 and Cu and SiO_2 and Zn, suggest that zinc and copper occur preferentially in chloritized, rather than in silicified rocks. FeO^T has a poor positive correlation with Cu and Zn; however, field observations of zinc and copper mineralization in outcrop, trenches and drill core show strong coincidence with iron sulphides (see 'Mineralization').

REE ANALYSIS

One sample (M-34) was submitted for REE analysis by INAA at Activation Laboratories Ltd., Brantford, Ontario. As noted in 'Lithology', flow rocks and intrusions were not positively identified in the map area. This sample represents a possible porphyry phase of 'two-quartz' rock (unit 2); the corresponding outcrop has a massive to pebbly texture, and the thin section contains only minor (0 to 5%) lithic fragments.

The REE pattern from this sample (Fig. 45) has a relatively flat HREE pattern, slightly steeper LREE pattern and negligible Eu anomaly. The REE patterns of other Amisk Group rhyolites from the Flin Flon area are similar, with relatively flat HREE patterns, slightly to markedly steeper LREE patterns, and negligible to negative Eu anomalies (Bailes and Syme, 1989); however, the concentrations of the individual elements are markedly lower for this sample.

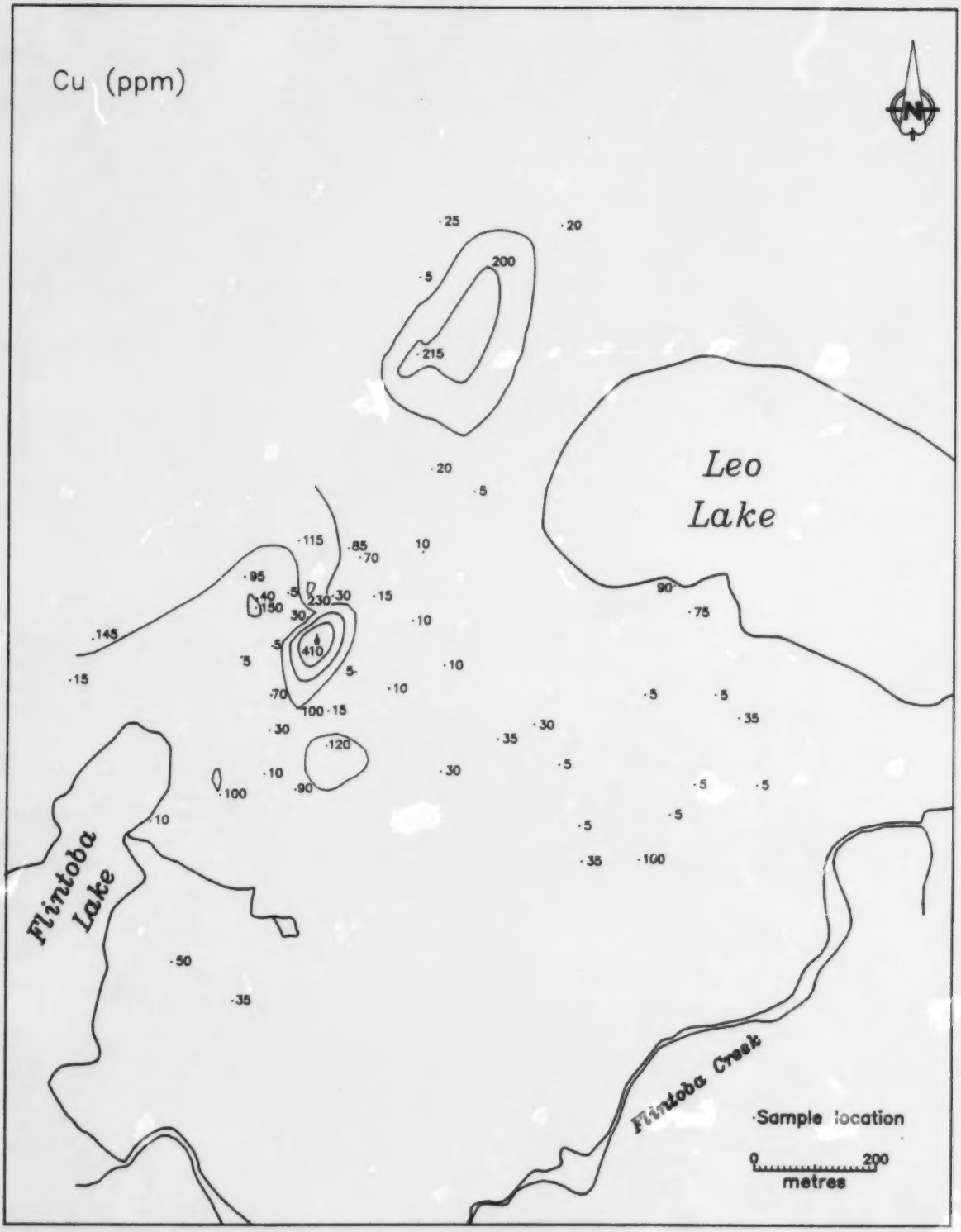

Figure 43: Contour map of Cu (ppm) concentrations. Contour interval = 100 ppm.

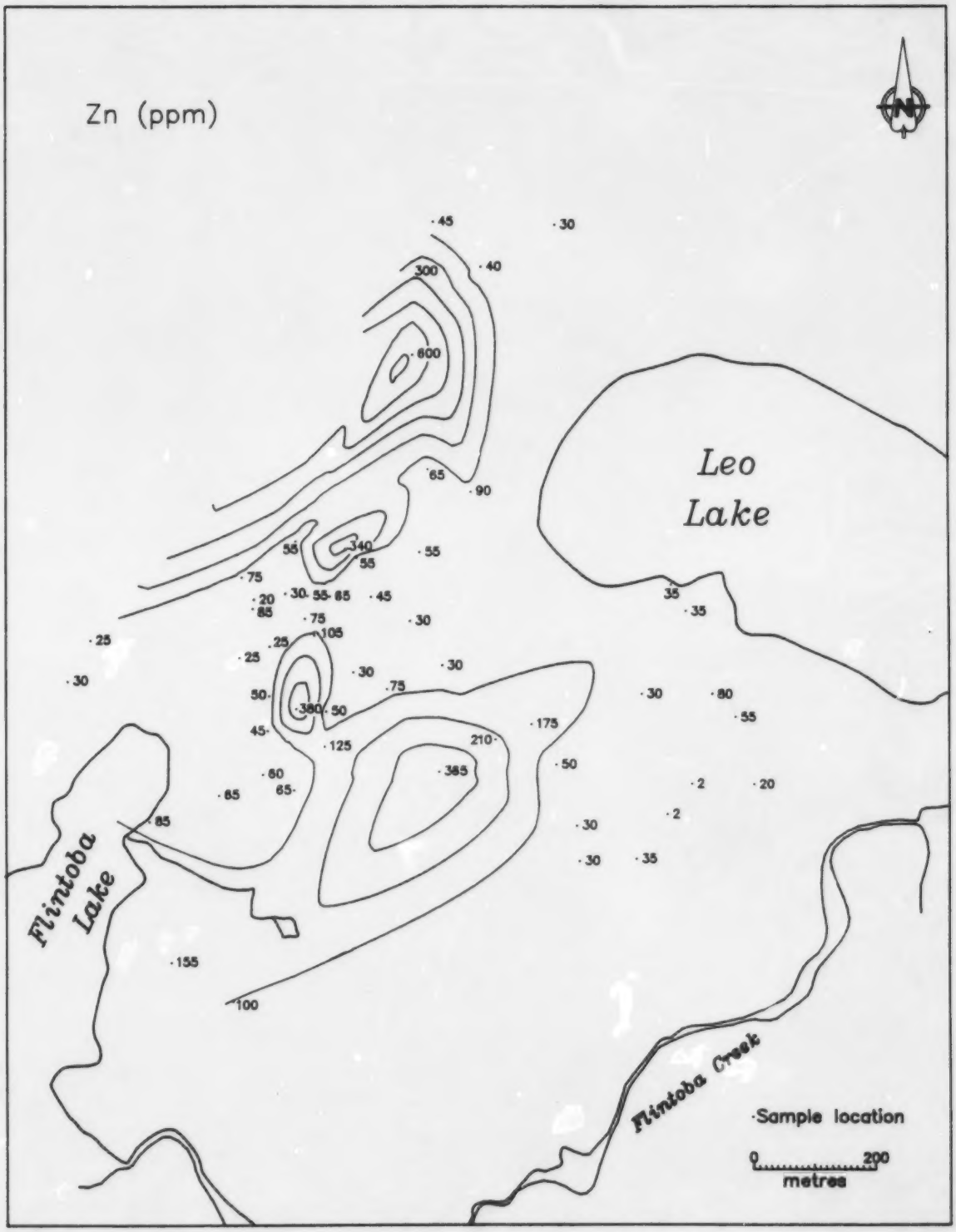

Figure 44: Contour map of Zn (ppm) concentrations. Contour interval = 100 ppm.

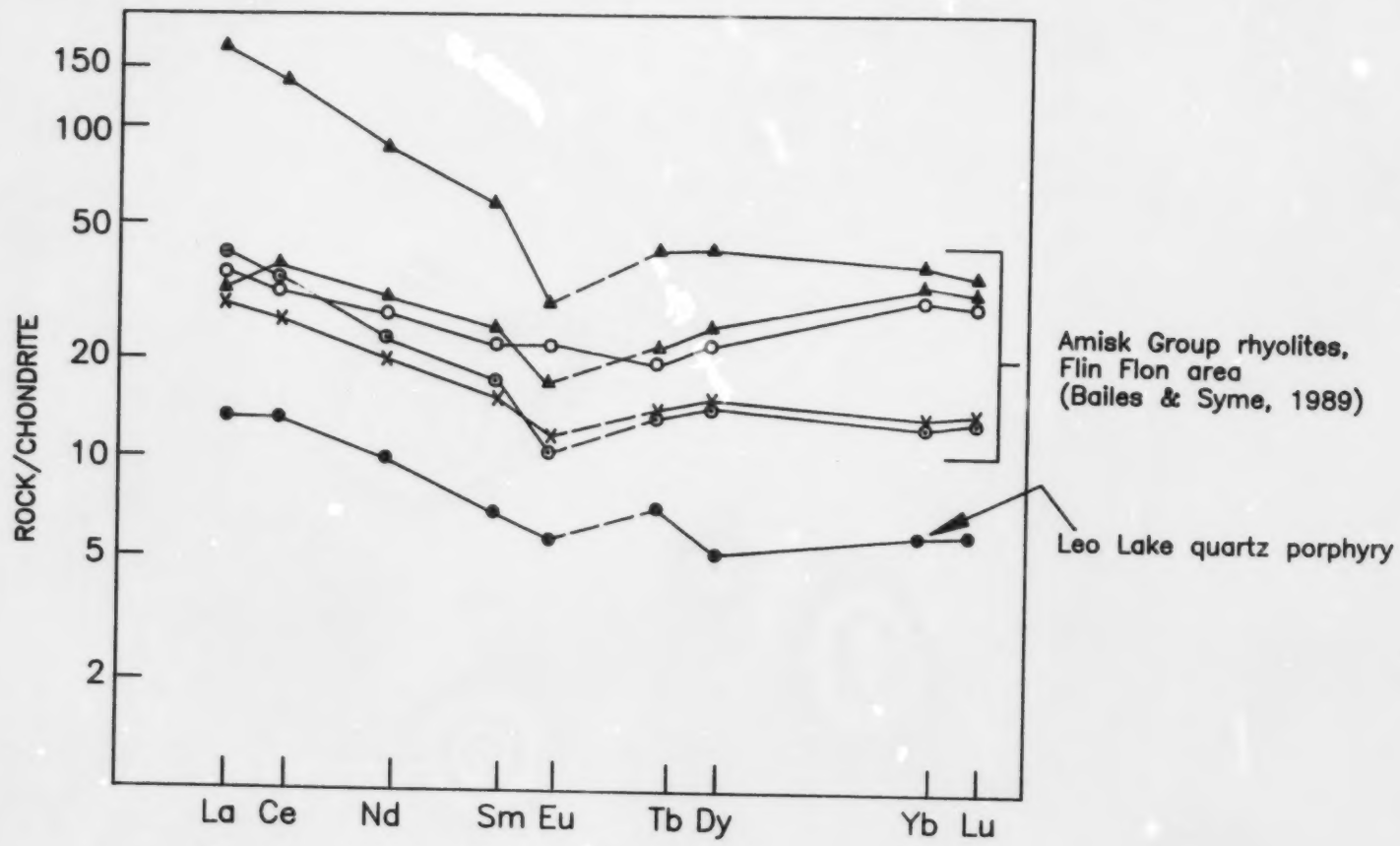

Figure 45: Chondrite normalized REE plot of porphyry phase of unit 2 (sample M-34). The upper five plots are for Amisk Group rhyolite samples from the Flin Flon area reported in Bailes and Syme (1989).

SUMMARY AND DISCUSSION

Since the project area represents a relatively small portion of the Baker Patton felsic complex, it is appropriate to summarize here only salient features from this mapping program. Larger discussions of facies analyses shall be withheld until the geological database for the entire felsic complex has been sufficiently detailed.

The Leo Lake area is characterized by dominantly fragmental and lesser massive, quartz-phyric and aphyric, rhyodacitic to rhyolitic volcanic rocks. Units distinguished within this map area have many similar lithologic features, and are discriminated on outcrop primarily on the basis of (a) the size, abundance and distribution of quartz phenocrysts, and by (b) the composition and size of lithic fragments. Volcanic textures have been poorly preserved and fragments are commonly difficult to distinguish because of extensive deformation and alteration. Layers are poorly sorted and unstratified, and are generally < 1 m thick. They are composed of heterolithic, angular (to rounded), nonvesicular, quartz- (and quartz-feldspar-) phyric and aphyric, matrix-supported ash, lapilli and blocks, and 0 to 20%, unimodally and bimodally distributed, broken quartz phenocrysts in an ash matrix. Major characteristics of fragments in units 1 through 4 are summarized in Table 8.

Pumice is tentatively identified only in a few locations. However, it is possible that compaction, devitrification, alteration and deformation destroyed or conceal additional pumice. Thin sections and etched slabs show streaked aggregates of sericite along prominent directions of cleavage; these could represent altered equivalents of eutaxitic fiamme, but may also strictly represent aligned alteration phenomena.

'Pseudo'-fragmental textures imposed by alteration were identified within the map area, notably where a chloritic matrix forms a network surrounding ovoid unaltered areas of felsic rock, and also where chlorite ± sericite ± pyrite form lenticular domains. Allen (1988) addressed the problem of false pyroclastic textures produced by devitrification, perlitic fracturing and hydrothermal alteration in flow and associated autoclastic felsic rocks. His main textural criteria used to differentiate true and false pyroclastic textures are summarized in Table 9, with an added synopsis of observations from this map area for comparison. Structural cleavages lend a pebbly texture to the rocks in outcrop, so additional caution must be exercised in this area to distinguish false fragments bounded by cleavage planes from true fragments that are elongated parallel to prominent cleavage plane(s).

The heterolithologic character of fragmental rocks indicates that the rocks are probably not autoclastic. The absence of flow margins and flow structures such as flow bands further contradict an extrusive flow origin for rocks in this map areas. The rocks are differentiated from high-level intrusive rocks by the lack of chilled margins, the lack of abundant spherulites and the abundance of lithic fragments. Spherulites and lithophysae were identified, but they are restricted in their extent and abundance, and are considered to be indicators of devitrification within fragmental units rather than components of flow or intrusive rocks. Parts of units 2 and 3 are mostly massive with only a small amount of lithic fragments; these parts may represent hypabyssal equivalents.

The fragmental rocks are interpreted to be pyroclastic because of the presence of (a) abundant broken euhedral quartz and plagioclase phenocrysts, and (b) dominantly subangular heterolithic fragments, of which one of the most abundant types is similar in composition to the matrix. Evidence of pumice (see above) and shards presumably has been obliterated. Fragments have not been significantly rounded or obviously weathered. However, many fragments are derived from previously consolidated fragmental material. The fragments may have been formed as the result of explosion(s) that disturbed fragmental material that had been previously deposited, perhaps as block-and-ash flows. Alternatively, the fragments may have been produced by brecciation of pre-existing fragmental strata along the front and sides of a progressive lava dome.

The Leo Lake area has potential for volcanogenic massive sulphide exploration. Because the bulk of the mineralization is lithologically restricted to unit 1, it is concluded that mineralization is synvolcanic. The effects of multiple stages of folding and faulting have been identified within the map area. The deformation has partly mobilized and focussed earlier synvolcanic mineralization along fractures and fold hinges.

The rocks have been chloritized and sericitized, but also pyritized, silicified, epidotized, carbonatized and saussuritized. Unit 1 is extensively altered, and is notably pyritized. Units 2, 3 and 4 are generally less intensely altered and pyrite is a comparatively minor (< 1%), late constituent.

Results of silicate whole rock analyses substantiate observations of alteration in outcrop. Rocks are enriched in SiO_2, FeO^T, MgO, Zn and Cu, hydrated, and depleted in CaO, Na_2O and K_2O. These results are attributed to alteration, notably chloritization, sodium and calcium depletion, and silicification. The results obtained here are typical of geochemical responses in volcanic rock associations that have undergone synvolcanic hydrothermal alteration (Govett and Nichol, 1979).

Some comparisons between the Leo Lake area and the Baker Patton area, 3 km to the southwest, may be made. Felsic rocks in the Baker Patton area are more diverse, comprising a variety of pyroclastic breccias and reworked pyroclastic rocks, flow rocks and their autoclastic breccias, a diatreme breccia, and lenses of quartz-rich tuff (Gale and Foote, 1988; Tannahill and Gale, 1986). The 'two-quartz' rhyolite appears to be similar to a lithologic unit that occurs in the Baker Patton area as an areally extensive reworked pyroclastic and flow rock (Tannahill and Gale, 1986). To date, this unit, despite morphological differences, is the only unit that warrants correlation between the two areas.

At the Baker Patton deposit, drill core and waste rocks contain solid sulphide mineralization. Crosscutting vein type mineralization hosted by altered dacite flows is exposed near the shaft; minor disseminated and mobilized vein type pyrite occurs both west and east of the shaft (Tannahill and Gale, 1986). In the Leo Lake area, solid and vein type sulphide mineralization is confined to unit 1 rocks. Minor disseminated and mobilized vein type pyrite is disseminated in other units.

Table 8

Summary of characteristics of felsic volcanic fragments from units 1 through 4

Unit 1	Unit 2	Unit 3	Unit 4
Heterolithic (to monolithic)	Heterolithic (to monolithic)	Monolithic (to heterolithic)	Heterolithic (to monolithic)
Juvenile dominant	Juvenile dominant	Juvenile dominant	Juvenile dominant
Cognate present	Cognate present	Cognate present	Cognate present
Quartz ± feldspar phyric, aphyric	Quartz ± feldspar phyric, aphyric	Quartz ± feldspar phyric, aphyric	Quartz ± feldspar phyric, aphyric
Generally nonvesicular	Generally nonvesicular	Generally nonvesicular	Generally nonvesicular
Ash dominant	Ash dominant	Ash dominant	Ash dominant
Lapilli, blocks common	Lapilli, blocks common	Lapilli, blocks present	Lapilli, blocks common
Angular (to rounded)	Angular (to rounded)	Rounded to angular	Angular (to rounded)
Pumice tentatively identified		Pumice tentatively identified	
Matrix supported	Matrix supported	Matrix supported	Matrix supported
Unstratified	Unstratified	Unstratified	Unstratified
Unsorted	Unsorted	Unsorted	Unsorted
Devitrified	Devitrification not apparent	Possibly devitrified	Devitrification not apparent

Table 9

Main textural criteria for distinguishing true felsic pyroclastic rocks from false pyroclastic rocks (from Allen, 1988) and synopsis of these criteria for the Leo Lake map area

False pyroclastic texture	True pyroclastic texture	Leo Lake area
Euhedral and subhedral phenocrysts; uniform porphyritic texture in 'matrix' and 'fragments'.	Euhedral and subhedral phenocrysts; uniform porphyritic texture in fiamme and lithic fragments; in matrix, crystals and crystal fragments range from 'dust' to phenocryst size.	Euhedral and subhedral phenocrysts; lithic fragments may contain porphyritic or broken crystals. Crystals are randomly distributed. Matrix contains broken crystals with size range from 'dust' to phenocryst size.
Cuspate and platy nonflattened 'shards' locally grade into relict perlitic texture.	Arcuate-cuspate nonflattened shards not associated with perlitic densely welded texture.	Shards not identified.
'Fiamme' with cuspate margins and layers in thin bedded 'tuff' defined by margins of interconnected bulbous to nodular devitrification or alteration structures.	Fiamme and tuff layers not defined by margins of bulbous to nodular structures.	Fiamme not identified. Layers in tuff not defined by margins of bulbous to nodular structures.
Relict flow banding within some phyllosilicate 'fiamme' and locally in 'matrix'.	Most do not exhibit flow banding.	Flow banding not identified.
Lithic inclusions are uncommon; but, (1) some flow rocks do contain lithic inclusions and (2) alteration may produce apparent lithics	Country rock and/or cognate lithics are rarely absent.	Cognate lithic fragments common. Some apparent alteration-produced lithic fragments identified.
Autoclastic breccias are monomictic, with flow banded and/or perlitic dense to poorly pumiceous fragments; grade locally into brecciated *in situ* flows with jigsaw clast relationships.	Breccias comprise highly pumiceous or denser phreatomagmatic or phreatic fragments; do not display jigsaw *in situ* breccia relationships.	Breccias are heterolithologic to monolithologic; do not display jigsaw *in situ* brecciation relationships.

ACKNOWLEDGEMENTS

This project was initiated and supervised by G.H. Gale and forms part of a detailed study of the Baker Patton felsic complex. Assistance in the field was provided by J. Mitchell and C. Graham. The 'M-' series samples were collected by R. Schmidtke. D.R. Eccles and D. Bagwell produced the geochemical contour maps and Autocad figures. Critical review by, and discussions with, D.A. Baldwin, M.A.F. Fedikow and G.H. Gale are greatly appreciated. E. Fluskey of Granges Incorporated permitted access to and sampling of drill core.

REFERENCES

Assessment Files 90427, 90435

Manitoba Energy and Mines, Minerals Division.

Allen, R.L.

1988: False pyroclastic textures in altered silicic lavas, with implications for volcanic-associated mineralization; Economic Geology, v. 83, p. 1424-1446.

Bailes, A.H.

1971: Preliminary compilation of the geology of the Snow Lake-Flin Flon-Sherridon area; Manitoba Mines and Natural Resources, Mines Branch, Geological Paper 1/71, 27 p.

Bailes, A.H. and Syme, E.C.

1989: Geology of the Flin Flon-White Lake area; Manitoba Energy and Mines, Geological Report GR87-1, 313 p.

Bailes, A.H., Syme, E.C., Galley, A., Price, D.P., Skirrow, R. and Ziehlke, D.J.

1987: Early Proterozoic volcanism, hydrothermal activity, and associated ore deposits at Flin Flon and Snow Lake, Manitoba; Geological Association of Canada-Mineralogical Association of Canada Joint Annual Meeting, 1987, Saskatoon, Saskatchewan, Field Trip Guidebook 1, 95 p.

Bateman, J.D. and Harrison, J.M.

1945: Mikanagan Lake; Geological Survey of Canada, Map 832A, 1:63 360.

Buckham, A.F.

1944: Athapapuskow Lake; Geological Survey of Canada, Map 807A, 1:63 360.

England, D.

1979: Petrology and chemistry of the volcanic rocks associated with the North Star copper deposit; University of Manitoba, B.Sc. Thesis (unpublished), 94 p.

Ferreira, K.J.

1987a: Geology of the Leo Lake area; In Manitoba Energy and Mines, Minerals Division, Report of Field Activities, 1987, p. 84-86.

Ferreira, K.J.

1987b: Geology of the Leo (Mud) Lake area; Manitoba Energy and Mines, Preliminary Map 1987-MI-1, 1:5 000.

Ferreira, K.J.

1988: Geology of the Leo Lake area; In Manitoba Energy and Mines, Minerals Division, Report of Field Activities, 1988, p. 72-76.

Gale, G.H. and Eccles, D.R.

1988: Mineral deposits and occurrences in the Flin Flon area NTS 63K/13: Part I, Mikanagan Lake area (63K/13SE); Manitoba Energy and Mines, Mineral Deposit Series, Report No. 1, 133 p.

Gale, G.H. and Foote, G.

1988: Geological setting of the Baker Patton alteration zone; In Manitoba Energy and Mines, Minerals Division, Report of Field Activities, 1988, p. 77-79.

Gordon, T.M., Hunt, P.A., Bailes, A.H. and Syme, E.C.

1990: U-Pb ages from the Flin Flon and Kisseynew belts, Manitoba: chronology of crust formation at an Early Proterozoic accretionary margin; In J.F. Lewry and M.R. Stauffer (*eds.*), The Early Proterozoic Trans-Hudson Orogen: lithotectonic correlations and evolution; Geological Association of Canada, Special Paper 37, p. 177-199.

Govett, G.J.S. and Nichol, I.

1979: Lithogeochemistry in mineral exploration; In Geophysics and geochemistry in the search for metallic ores (P.J. Hood, *ed.*); Geological Survey of Canada, Economic Geology Report 31, p. 339-362.

Hayden-Luck, D. and Gale, G.H.

1985: Geological investigations in the Baker Patton-Centennial Mine area; In Manitoba Energy and Mines, Geological Services, Mines Branch, Report of Field Activities, 1985, p. 74-76.

Hudson Bay Mining and Smelting Company Limited, Geological Staff

1957: North Star and Don Jon Mines, Cuprus Mine, Schist Lake Mine; In Structural Geology of Canadian Ore Deposits, Volume II, Canadian Institute of Mining and Metallurgy, p. 247-262.

Kalliokoski, J.

1953: Weldon Bay, Manitoba; Geological Survey of Canada, Map 1020A, 1:63 360.

Le Maitre, R.W.

1976: The chemical variability of some common igneous rocks; Journal of Petrology, v. 17, p. 589-637.

Mineral Inventory Card 63K/13SE Cu10

Manitoba Energy and Mines, Minerals Division.

Mwanang'Onze, E.H.B.

1978: Stratigraphy and petrochemistry of the host rocks of copper-zinc deposits in the Flin Flon-Snow Lake greenstone belt; University of Manitoba, Ph.D. Thesis (unpublished), 420 p.

Stauffer, M.R., Mukherjee, A.C. and Koo, J.

1975: The Amisk Group: an Aphebian(?) island arc deposit; Canadian Journal of Earth Sciences, v. 12, p. 2021-2035.

Tannahill, B. and Gale, G.H.

1986: Geology of the Baker Patton area; In Manitoba Energy and Mines, Minerals Division, Report of Field Activities, 1986, p. 65-67.

Tanton, T.L.

1941: Flin Flon; Geological Survey of Canada, Map 632A, one inch equals one mile.

Wright, J.F.

1931: Geology and mineral deposits of a part of northwest Manitoba; Geological Survey of Canada, Summary Report 1930, Part C, 131 p.

APPENDIX I

MAJOR ELEMENT ANALYSES, LEO LAKE AREA

Lab Numbers	Sample Numbers	UTM Northing	UTM Easting	SiO_2 %	Al_2O_3 %	FeO^T %	CaO %	MgO %	Na_2O %	K_2O %	TiO_2 %	P_2O_5 %	MnO %	LOI %	CO_2 %	TOTAL %
872447	LEO-213-2	6076686	721355	70.1	13.8	1.78	2.07	2.36	5.73	0.73	0.3	0.06	0.03	2.9	NA	99.87
882897	LEO-263-1	6076686	721355	72.9	14.67	0.94	0.74	0.42	5.00	2.79	0.1	0.05	0.04	1.8	0.45	99.42
882898	LEO-263-2	6076554	720544	65.1	14.13	5.62	0.34	5.23	1.11	2.59	0.3	0.07	0.07	4.1	0.47	98.68
882899	LEO-263-3	6076557	720552	78.4	11.68	0.59	0.31	0.99	0.78	3.62	0.3	0.06	0.02	2.3	0.57	99.07
882892	LEO-334-1	6075961	721130	74.1	12.43	4.80	0.08	1.45	0.49	3.19	0.3	0.08	0.05	2.5	NA	99.47
882890	LEO-343-1	6075918	720800	67.5	12.88	6.83	1.17	2.20	0.68	3.76	0.4	0.16	0.07	3.6	NA	99.23
882889	LEO-346-1	6075741	721184	70.7	12.19	6.06	0.64	2.93	2.51	1.13	0.3	0.09	0.08	3.1	NA	99.76
882891	LEO-347-1	6075758	721048	73.7	12.80	4.27	0.31	1.51	1.97	2.50	0.3	0.09	0.05	2.2	NA	99.73
882888	LEO-350-1	6076021	720965	58.4	15.31	6.56	1.13	7.13	1.78	2.98	0.3	0.08	0.06	5.5	NA	99.27
882894	LEO-510-1	6077438	721122	80.1	10.34	0.29	1.58	0.42	4.76	0.34	0.3	0.07	0.01	1.5	NA	99.66
882893	LEO-518-1	6077502	721216	66.9	14.23	5.91	1.05	2.78	1.62	2.60	0.4	0.12	0.13	3.2	NA	98.93
882895	LEO-520-1	6077617	721173	68.3	13.34	5.24	1.79	1.77	4.86	0.92	0.4	0.12	0.09	1.9	NA	98.75
870866	M-01	6076422	721101	76.0	10.5	3.17	0.00	3.86	0.27	1.88	0.3	0.07	0.03	3.2	NA	99.28
881654	M-02	6076422	721101	72.1	11.27	5.15	0.29	4.64	0.21	1.69	0.3	0.05	0.16	3.7	NA	99.55
881655	M-04	6076410	720614	73.9	10.46	7.16	0.09	2.77	0.26	1.27	0.3	0.07	0.04	3.2	NA	99.48
881656	M-06	6076451	720671	71.7	11.86	5.36	0.14	3.97	0.25	1.86	0.3	0.09	0.11	3.8	NA	99.47
881657	M-07	6076381	720719	72.0	11.62	5.63	0.54	3.02	0.35	2.50	0.3	0.08	0.08	3.8	NA	99.93
870841	M-08	6076446	720722	71.0	10.9	4.71	1.18	2.79	3.40	0.92	0.3	0.07	0.11	3.8	NA	99.18
870842	M-10	6076487	720834	72.1	10.8	4.81	0.20	3.93	0.24	2.07	0.3	0.09	0.07	3.6	NA	98.21
881658	M-11	6076531	720936	72.8	12.83	4.11	0.17	3.21	0.39	2.62	0.3	0.09	0.02	3.3	NA	99.88
870843	M-13	6076567	720618	76.5	10.7	1.42	0.76	3.27	0.38	2.63	0.2	0.04	0.02	3.9	NA	99.82
870844	M-14	6076618	720683	66.5	14.1	3.42	1.57	4.02	3.72	1.23	0.2	0.06	0.05	4.1	NA	98.97
870845	M-15	6076661	720688	73.8	10.6	5.51	0.46	1.71	3.27	1.04	0.3	0.06	0.07	2.7	NA	99.52
870846	M-16	6076748	720758	72.4	10.9	5.57	0.16	3.76	0.78	1.79	0.3	0.08	0.11	3.5	NA	99.35
870847	M-17	6076660	720729	70.9	11.2	6.61	0.25	3.42	2.05	0.86	0.3	0.09	0.09	3.4	NA	99.17
870848	M-18	6076587	720700	65.9	13.9	4.95	0.53	5.38	2.45	1.46	0.1	0.06	0.04	4.3	NA	99.07
881659	M-19	6076518	720772	76.4	11.90	2.41	0.09	2.80	0.32	2.59	0.2	0.05	0.01	3.1	NA	99.89
870849	M-20	6076614	720877	73.1	10.5	4.16	0.13	4.53	0.28	1.81	0.3	0.06	0.02	3.7	NA	98.59
870850	M-21	6076742	720895	74.4	10.7	4.70	0.01	3.48	0.33	1.68	2.0	0.04	0.05	3.4	NA	100.79
870851	M-22	6076732	720779	72.3	11.0	5.54	0.07	3.47	2.03	0.98	0.3	0.09	0.06	3.0	NA	98.84
881652	M-23	6076659	720805	71.0	10.9	5.84	0.33	3.83	1.55	1.09	0.3	0.09	0.07	3.6	NA	98.60
870853	M-24	6076475	720617	63.8	13.8	5.26	1.66	4.21	2.34	1.82	0.4	0.07	0.04	5.3	NA	98.70
870854	M-25	6076546	720562	74.4	11.2	1.16	0.80	3.05	4.06	1.05	0.3	0.08	0.03	2.8	NA	98.93
870855	M-26	6076654	720589	81.0	9.4	0.68	0.61	1.06	4.19	0.80	0.2	0.06	0.02	1.7	NA	99.72
870856	M-27	6076637	720587	68.4	13.4	3.12	0.60	4.33	3.03	1.70	0.2	0.06	0.04	3.7	NA	98.58
870857	M-28	6076695	720567	67.7	11.3	5.63	0.92	5.27	0.83	1.37	0.3	0.06	0.04	5.1	NA	98.52
870858	M-29	6076762	720666	73.7	9.6	6.05	0.03	2.46	0.23	1.80	0.3	0.08	0.02	3.4	NA	97.67
870859	M-30	6076665	720647	67.2	13.5	4.00	2.38	1.88	5.43	0.33	0.3	0.07	0.03	3.5	NA	98.62
881660	M-31	6076254	721352	78.9	8.48	4.82	0.12	2.89	0.16	1.21	0.2	0.06	0.03	2.8	NA	99.68
881661	M-32	6076310	721397	72.9	12.62	5.02	0.23	2.17	3.55	1.00	0.3	0.08	0.04	2.4	NA	100.32
881662	M-33	6076309	721512	78.0	11.00	1.88	0.21	1.32	4.56	0.73	0.3	0.05	0.02	1.6	NA	99.66
881663	M-34	6076680	721359	72.8	12.73	2.02	1.43	2.18	4.18	1.11	0.3	0.04	0.03	3.0	NA	99.81

881664	M-35	6076631	721386	70.0	13.24	3.01	2.45	2.30	4.31	0.80	0.3	0.06	0.04	3.5	NA	100.02
881665	M-36	6076477	721435	69.6	12.68	5.06	0.27	4.03	2.11	1.33	0.3	0.06	0.06	3.5	NA	99.01
881666	M-37	6076434	721478	68.7	13.36	4.37	0.97	4.40	2.48	1.34	0.3	0.07	0.07	3.9	NA	99.98
881667	M-38	6076347	721147	74.4	10.24	5.12	0.12	4.28	0.23	1.08	0.3	0.08	0.05	3.5	NA	99.37
870867	M-39	6076478	721305	74.1	10.7	6.07	0.03	3.14	0.19	1.56	0.2	0.07	0.05	3.2	NA	99.31
870860	M-40	6076233	721185	73.1	10.6	5.17	0.03	4.37	0.24	1.36	0.2	0.07	0.03	3.5	NA	98.67
881668	M-41	6076167	721190	68.8	11.34	8.88	0.12	4.62	0.14	1.14	0.4	0.07	0.06	3.8	NA	99.33
881669	M-42	6076171	721295	73.0	11.83	5.43	0.43	1.64	4.62	0.30	0.3	0.08	0.05	2.0	NA	99.66
881670	M-43	6076394	721034	74.2	10.30	4.30	0.58	3.81	0.27	1.86	0.3	0.05	0.14	3.7	NA	99.49
870861	M-44	6076334	720930	74.3	11.0	4.46	0.09	3.92	0.25	2.11	0.2	0.06	0.12	3.5	NA	100.01
870862	M-45	6076329	720605	69.1	11.9	8.12	0.00	4.15	0.23	1.15	0.3	0.08	0.07	4.0	NA	99.10
870863	M-46	6076290	720524	77.5	11.1	3.65	0.28	1.71	0.75	1.49	0.3	0.07	0.03	2.7	NA	99.58
870865	M-50	6076300	720662	71.4	11.1	6.21	0.06	4.08	0.38	0.94	0.3	0.09	0.05	3.9	NA	98.51
870794	M-52	6076896	720910	71.6	13.5	3.05	0.24	1.78	3.94	2.07	0.3	0.06	0.04	2.0	NA	98.58
870796	M-54	6076854	720989	73.7	11.0	3.98	0.08	2.95	2.56	1.60	0.2	0.05	0.07	2.4	NA	98.59
870797	M-55	6077109	720883	67.5	11.7	6.69	0.40	4.56	0.31	2.01	0.3	0.09	0.21	3.8	NA	97.57
870798	M-56	6077253	720887	71.3	11.8	5.44	0.23	2.74	2.41	1.30	0.4	0.09	0.18	2.6	NA	98.49
870800	M-58	6077273	721010	73.7	11.1	3.56	0.50	2.18	3.26	1.02	0.3	0.08	0.05	2.1	NA	97.85
870864	M-59	6077470	721283	71.3	11.7	7.27	0.32	3.08	0.29	1.66	0.3	0.07	0.09	3.5	NA	99.58
870801	M-60	6077351	721147	70.2	12.7	3.95	2.03	2.53	3.21	1.19	0.4	0.12	0.03	2.5	NA	98.86
870802	M-61	6076241	720396	70.8	12.6	4.86	0.47	2.16	0.69	2.08	0.4	0.12	0.03	3.4	NA	97.61
870803	M-62	6076578	720287	68.9	12.3	7.68	0.41	1.27	2.61	1.48	0.4	0.12	0.08	2.4	NA	97.65
870805	M-64	6076502	720245	68.2	12.0	7.04	1.39	2.04	3.80	0.44	0.4	0.19	0.05	2.6	NA	98.15
870806	M-73	6075979	720435	66.0	11.4	5.92	2.25	2.49	2.76	2.09	0.3	0.11	0.07	4.8	NA	98.19
870807	M-75	6075907	720549	69.5	10.5	4.64	1.95	2.37	2.53	3.05	0.3	0.10	0.05	4.4	NA	99.39

Note - All percentages refer to weight per cent.

NA - Not analyzed.

APPENDIX II

COPPER AND ZINC ANALYSES, FELSIC VOLCANIC ROCKS, LEO LAKE AREA

Lab Numbers	Sample Numbers	Cu ppm	Zn ppm
800112	M-01	30	230
800113	M-02	40	175
800115	M-04	30	45
800117	M-06	100	380
800118	M-07	120	125
800119	M-08	15	50
800121	M-10	10	75
800122	M-11	10	30
800124	M-13	5	25
800125	M-14	30	75
800126	M-15	230	55
800127	M-16	85	340
800128	M-17	30	65
800129	M-18	410	105
800130	M-19	5	30
800131	M-20	10	30
800132	M-21	10	55
800133	M-22	70	55
800134	M-23	15	45
800135	M-24	70	50
800136	M-25	5	25
800137	M-26	40	20
800138	M-27	150	85
800139	M-28	95	75
800140	M-29	115	55
800141	M-30	5	30
800142	M-31	5	2
800143	M-32	5	2
800144	M-33	5	20
800145	M-34	90	35
800146	M-35	75	35
800147	M-36	5	80
800148	M-37	35	55
800149	M-38	5	50
800150	M-39	5	30
800151	M-40	5	30
800152	M-41	35	30
800153	M-42	100	35
800154	M-43	35	210
800155	M-44	30	365
800156	M-45	10	60
800157	M-46	100	65
800161	M-50	90	65
810171	M-51	65	150
810172	M-52	20	65
810174	M-54	5	90
810175	M-55	215	600
810176	M-56	5	300
810177	M-57	25	45
810178	M-58	200	40
810179	M-60	20	30
810180	M-61	10	85
810181	M-62	145	25

APPENDIX II Continued

COPPER AND ZINC ANALYSES, FELSIC VOLCANIC ROCKS, LEO LAKE AREA

Lab Numbers	Sample Numbers	Cu ppm	Zn ppm
810182	M-63	155	125
810183	M-64	15	30
810192	M-73	50	155
810194	M-75	35	100

LEGEND

INTRUSIVE ROCKS

6 Granodiorite

5 Gabbro
- a epidotized
- b magnetite-bearing
- c quartz-bearing
- d magnetite-quartz-feldspar-amphibole rock

FELSIC VOLCANIC ROCKS

4 Fragmental Rhyodacite-Rhyolite, 5-20% unimodally distributed quartz phenocrysts
- a tuff
- b lapilli tuff
- c tuff breccia
- d chloritic tuff

3 Massive (to Fragmental) Rhyodacite-Rhyolite, <2% quartz phenocrysts
- a tuff
- b lapilli tuff

2 'Two-quartz' Fragmental Rhyodacite-Rhyolite, 5-25% bimodally distributed quartz phenocrysts
- a tuff
- b lapilli tuff
- c tuff breccia
- d quartz-plagioclase porphyry

1 Fragmental Rhyolite, rusty weathered, <5% quartz phenocrysts
- a tuff
- b lapilli tuff
- c tuff breccia
- d chloritic tuff

SYMBOLS

- Outcrop
- Lithologic contact, known, assumed
- Fault, approximate
- Antiform, axial trace, assumed
- Synform, axial trace, assumed
- Bedding; inclined, vertical, dip unknown
- Foliation (S_1); inclined, vertical, dip unknown
- Cleavage (S_2); inclined, vertical, dip unknown
- Trace of Fracture Cleavage (S_3)
- Trace of Schistosity
- Joint, inclined, vertical
- Trail, foot portage
- Trail, tractor
- Swamp
- Creek
- Trench

pond

Leo Lake

101°33'30"

54°47'30"

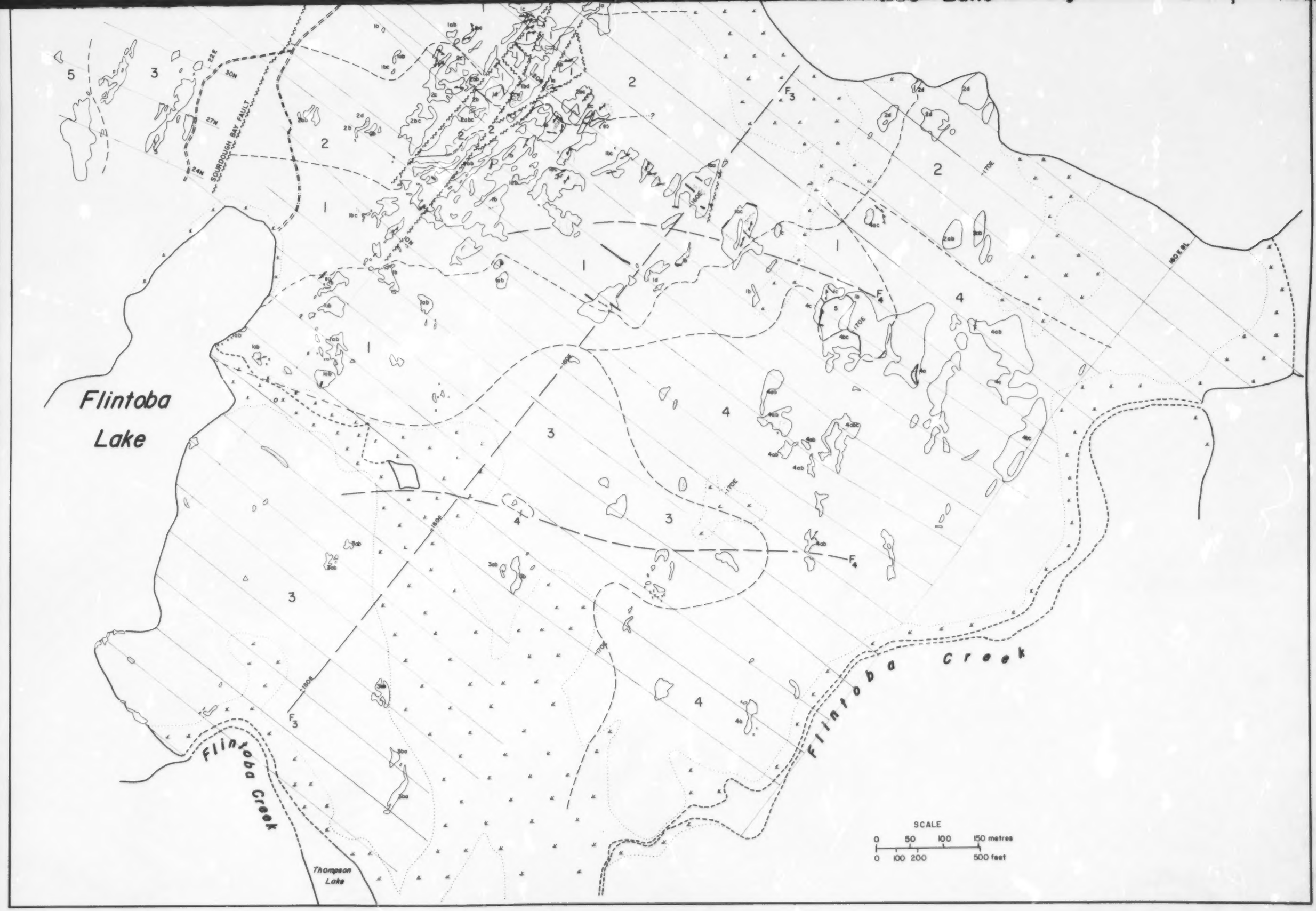

FIGURE 3: GEOLOGY OF THE LEO LAKE AREA

N
150 E BL
140E
160E
170E
60N
50N
40N
30N
27N
22E
LEO-520-1
LEO-519-1
M-58
M-60
LEO-510-1
M-59
M-56
M-55
M54
M52
M51
M50
M16
M22
M21
M28
M36
M27
M30
M15
M17
M23
M14
M13
M18
M20
M12
LEO-263-1
LEO-263-2
LEO-263-3
M24
M34
LEO-213-2
M35
pond
Leo Lake

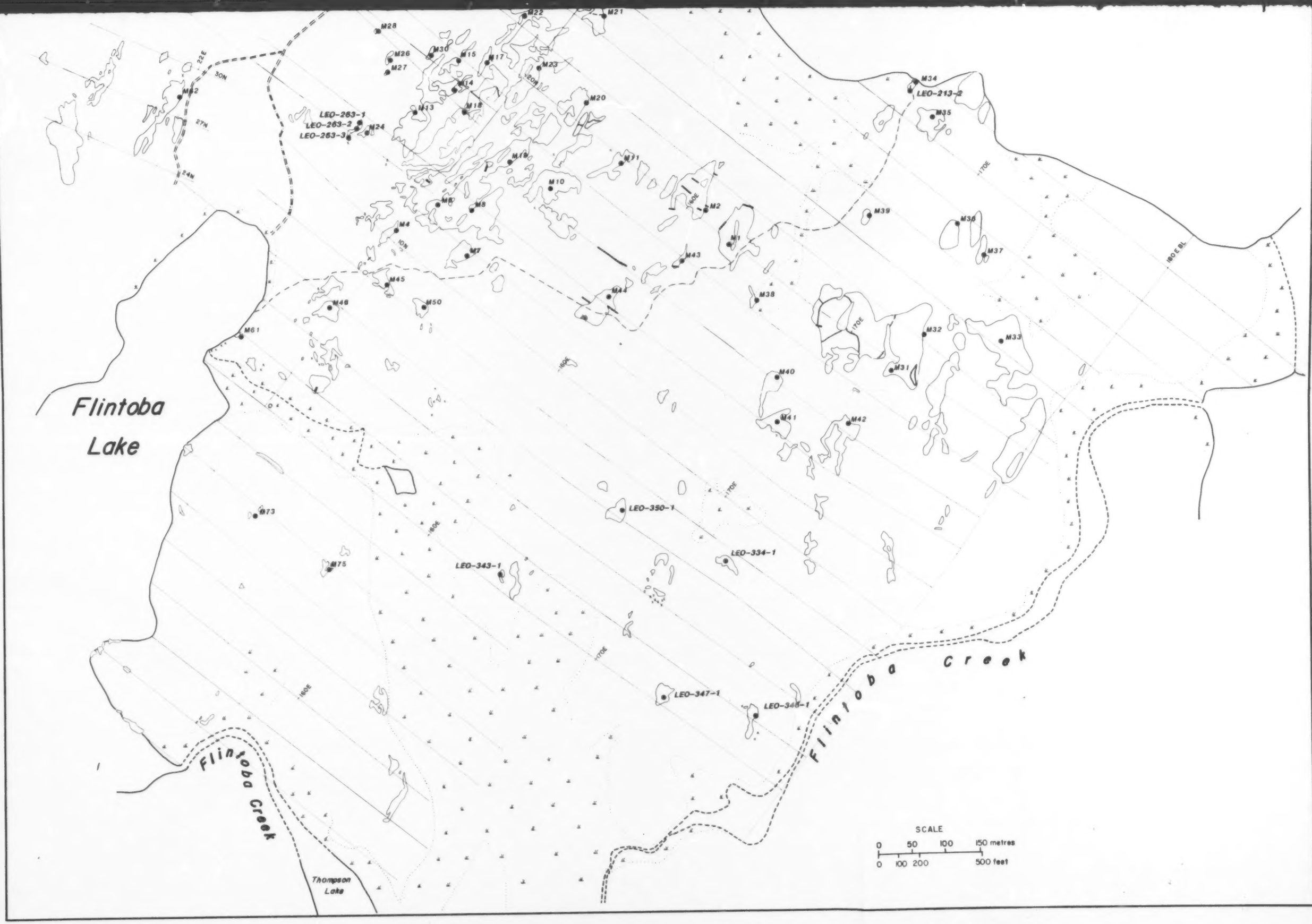

FIGURE 38: SAMPLE LOCATIONS OF ROCK GEOCHEMICAL ANALYSES